CATAL. REV.—SCI. ENG., 39(4), 345–393 (1997)

Brønsted Acid Sites in Zeolites Characterized by Multinuclear Solid-State NMR Spectroscopy

MICHAEL HUNGER

Institute of Chemical Technology I
University of Stuttgart
D-70550 Stuttgart, Germany

Downloaded By: [University of Stuttgart] At: 16:06 10 September 2009

I. INTRODUCTION 347

II. BACKGROUND OF SAMPLE PREPARATION 348
A. Preparation of Samples in Glass Ampoules 348
B. Technique of in Situ Injection 349

III. ^{1}H NMR SIGNALS OF HYDROXYL GROUPS IN DEHYDRATED ZEOLITES 350
A. Chemical Shifts 350
B. Residual Linewidth 353

IV. FORMATION OF HYDROXYL GROUPS IN ZEOLITES AND THEIR DEHYDROXYLATION 356
A. Formation by Ammonium Exchange 356
B. Mechanism of Hirschler and Plank 358
C. Dehydroxylation and Realumination of Zeolites 359

V. ACID STRENGTH OF HYDROXYL GROUPS IN CALCINED ZEOLITES 360
A. General Remarks 360
B. Adsorbate-Induced Chemical Shift 361

Copyright © 1997 by Marcel Dekker, Inc.

VI. ACCESSIBILITY AND LOCATION OF HYDROXYL GROUPS IN ZEOLITES 364
A. Application of Probe Molecules 364
B. Sophisticated Pulse Experiments 365

VII. MOBILITY OF HYDROXYL PROTONS 368
A. Theoretical Description 368
B. Experiments 370

VIII. LOCAL STRUCTURE OF BRIDGING HYDROXYL GROUPS .. 372
A. Internal H–Al Distance of Bridging OH Groups 372
B. Flexibility of the Local Structure 374

IX. FORMATION OF ADSORBATE COMPLEXES IN ACIDIC ZEOLITES 377
A. Adsorption of Methanol on HZSM-5 377
B. Influence on the Local SiOHAl Structure 381

X. IN SITU INVESTIGATIONS OF REACTIONS CATALYZED BY BRØNSTED ACID SITES 383
A. General Remarks 383
B. Reactions Catalyzed by Acidic Zeolites 384

XI. CONCLUDING REMARKS 386

NOTATION 387

ACKNOWLEDGMENTS 388

REFERENCES 388

Key Words: Zeolites; Brønsted acid sites; Bridging OH groups; Local structure; Solid-state NMR spectroscopy.

Downloaded By: [University of Stuttgart] At: 16:06 10 September 2009

ABSTRACT

Nearly all atoms contributing to the local structure of Brønsted acid sites in zeolites exhibit isotopes accessible for multinuclear solid-state nuclear magnetic resonance (NMR) investigations. Therefore, in the last 15 years, NMR spectroscopy has found numerous applications for the determination of the types of hydroxyl proton in zeolites, of their concentration, accessibility, and mobility, and for the characterization of their acid strength and local structure. It allows the study of the role of hydroxyl groups in the formation of adsorbate complexes and in heterogeneously catalyzed reactions. Meanwhile, NMR spectroscopy belongs to the most powerful techniques for the characterization of Brønsted acid sites in zeolites and related materials. The basis of this success is the invention of new sample preparation techniques, external magnetic fields with high-flux densities, effective line-narrowing methods, and

new two-dimensional experiments, making the detection of highly resolved solid-state NMR spectra and the separation of spectral parameters possible. This article gives a review of these techniques and a summary of the most important applications of multinuclear solid-state NMR spectroscopy for the characterization of Brønsted acid sites in dehydrated zeolites.

I. INTRODUCTION

Hydroxyl groups in zeolites may act as proton donor sites (Brønsted acid sites) which are responsible for the ability of zeolites to catalyze chemical reactions [1–5]. The characterization of hydroxyl groups is, therefore, an important prerequisite for catalyst tailoring. In the variety of experimental techniques which are used for the characterization of crystalline aluminosilicate and silicoaluminophosphate molecular sieves, nuclear magnetic resonance (NMR) spectroscopy possesses the benefit of providing detailed information on local bonds and solid-state interactions. In the last 15 years, this spectroscopic method was applied to investigate the zeolitic host, catalytic active centers, and adsorbed probe molecules, as well as their mutual chemical interactions. The present article gives a review of multinuclear solid-state NMR investigations of Brønsted acid sites in zeolites. Considering the local structure of bridging OH groups, nearly all atoms contributing to these Brønsted acid sites can be detected by NMR spectroscopy (Fig. 1). Its application allows the determination of the number of framework aluminum atoms in the next-nearest coordination sphere of T atoms and the mean Si–O–T bond angle (^{29}Si NMR) or the oxygen coordination of aluminum atoms and the geometry of framework AlO_4 tetrahedra (^{27}Al NMR). By ^{1}H and ^{2}H NMR spectroscopy, the concentration, acid strength, and mobility of Brønsted acid sites and atom–atom distances in the local SiOHAl structure (dipolar ^{1}H–^{27}Al interaction) can be derived. The chemical interactions of these OH groups with adsorbate molecules or reactants is studied by ^{13}C, ^{2}H, and ^{1}H NMR spectroscopy.

First, ^{1}H MAS (magic angle spinning) NMR investigations of hydroxyl groups in dehydrated zeolites were carried out with single-pulse excitation and in a magnetic field with a magnetic flux density of $B_0 = 1.4$ T, yielding signals with residual linewidths of about 1 kHz [6]. Application of external magnetic fields with magnetic flux densities of $B_0 \geq 7$ T and of the CRAMPS (Combined Rotational and Multiple-Pulse Spectroscopy) [7] or MAS technique with sample spinning rates of $\nu_{rot} \geq 10$ kHz [8,9] results in well-resolved ^{1}H MAS NMR spectra of dehydrated zeolites comparable to those of infrared (IR) spectroscopy. However, such investigations have to be carried out on carefully dehydrated samples, sealed in symmetric glass ampoules or filled in gastight rotors [6,7].

Downloaded By: [University of Stuttgart] At: 16:06 10 September 2009

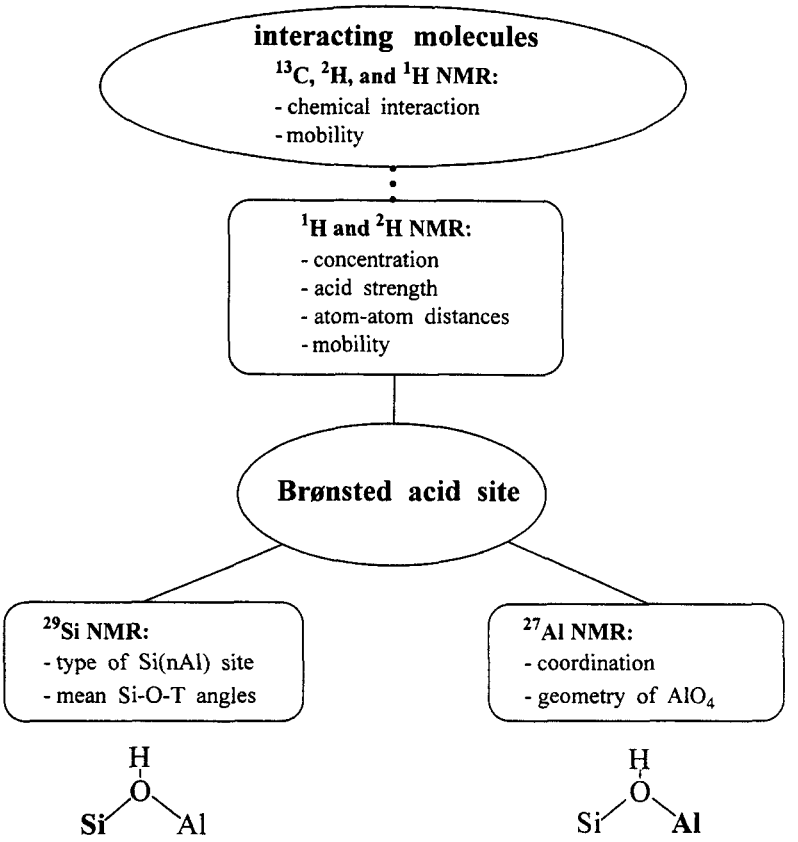


FIG. 1. Data and parameters derived by multinuclear solid-state NMR spectroscopy of bridging OH groups in zeolites.

Downloaded By: [University of Stuttgart] At: 16:06 10 September 2009

II. BACKGROUND OF SAMPLE PREPARATION

A. Preparation of Samples in Glass Ampoules

The application of solid-state NMR spectroscopy for the study of hydroxyl groups in zeolites requires a complete dehydration of the powder material. Often, samples calcined in an external furnace and sealed in glass tubes are used. In most cases, these samples are studied at room temperature without or after adsorption of probe molecules. Although first NMR investigations have been carried out without application of high-resolution solid-state techniques [10], in the beginning of the 1980's the MAS technique has been introduced which improved significantly the spectral resolution. To open the way for MAS NMR and CRAMPS NMR studies, new techniques for the preparation of calcined samples fused in glass tubes were developed. Figure 2 shows the scheme of a glass turning lathe applied for the preparation of symmetric glass ampoules. The glass tube is fixed by two chucks which rotate

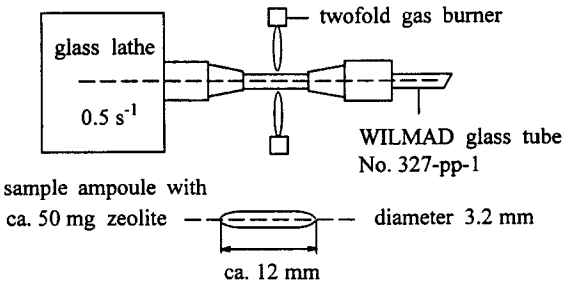


FIG. 2. Equipment for the preparation of calcined samples fused in symmetric glass ampoules.

Downloaded By: [University of Stuttgart] At: 16:06 10 September 2009

with a rate of ~0.5 s^{-1}. For a 4-mm Bruker DB MAS NMR probe, glass tubes produced by Wilmad Glass Company (No. 327-pp-1) are used. Applying a twofold gas burner, the glass tube is closed on the bottom. Then a waist with an inner diameter of ~1 mm is made at a distance of ~12 mm from the bottom. An alternative method is the application of commercial Pyrex glass inserts for MAS NMR rotors [11]. In the glass ampoules, about 50 mg of zeolitic powder material is calcined in vacuum and at temperatures up to 723 K. After calcination and adsorption of probe molecules, the glass ampoules are fused at the waist. To prevent a heating of the sample, the glass ampoule is clamped in one of the chucks and cooled by liquid nitrogen.

B. Techniques of in Situ Injection

Recently, new methods for the pretreatment and loading of zeolites inside the NMR spectrometer were developed [12–15]. Using modified MAS NMR probes, the zeolite powder is exposed to a continuous-flow carrier gas. The in situ equipment shown in Fig. 3 (top) is based on a commercial 7-mm Bruker DB MAS NMR probe [12–14]. An injection tube fixed by a support is axially placed in the center of the MAS rotor. Prior to the in situ MAS NMR investigations, about 300 mg of zeolite powder is filled into the MAS rotor. With a special tool, an axial hole is pressed into the powder material, resulting in an annular catalyst bed. Before starting the sample spinning, the injection tube is carefully inserted into the rotor. During the measurements, the spinning rotor is heated via the bearing gas of the MAS NMR turbine. Figure 3 (bottom) shows the carrier gas supply system [13,14]. Using a saturator, the carrier gas is loaded with adsorbate or reactant molecules. After injection of the carrier gas into the MAS rotor, it flows inside the rotor from bottom to top and leaves the rotor via an annular gap in the rotor cap. The temperature inside the MAS rotor is calibrated using the ^{207}Pb MAS NMR shift of $Pb(NO_3)_2$ as an internal thermometer [16]. The temperature gradient, ΔT, over the whole sample room inside the MAS rotor can be determined by the line broadening of the ^{207}Pb MAS NMR signal. The above-mentioned in

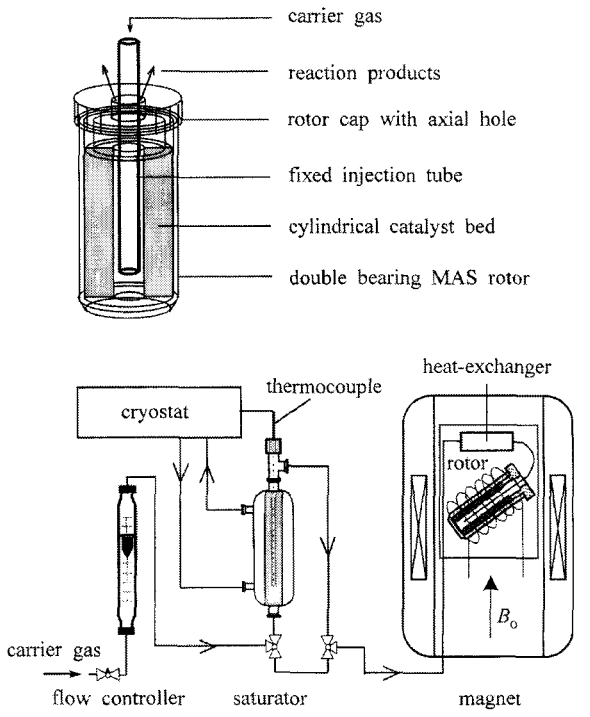


FIG. 3. Design of the MAS NMR rotor modified for in situ MAS NMR investigations under continuous-flow conditions (top) and the design of the educt supply system (bottom). (From Refs. 12 and 13.)

situ MAS NMR equipment allows the study of adsorbate complexes and of reactions catalyzed by Brønsted acid sites in zeolites under atmospheric pressure and in a temperature range limited by the heating system of the MAS NMR probe [13,14].

III. ^{1}H NMR SIGNALS OF HYDROXYL GROUPS IN DEHYDRATED ZEOLITES

A. Chemical Shifts

The ^{1}H MAS NMR signals of hydroxyl protons in dehydrated zeolites cover a range of chemical shifts from 0 to 7 ppm (Fig. 4) [9]. Silanol groups (SiOH) at the external surface of the zeolite particles and at framework defects have chemical shifts of 1.2–2.2 ppm (Fig. 4a). The lowest chemical shifts of hydroxyl protons in zeolites have been observed for undisturbed metal OH groups (MeOH) (Fig. 4b) (e.g., for OH groups on Mg^{2+} cations in zeolite Y) which are located in supercages and have a resonance position of ~0 ppm [17]. CaOH groups locked in the sodalite cages of dehydrated zeolite

Downloaded By: [University of Stuttgart] At: 16:06 10 September 2009

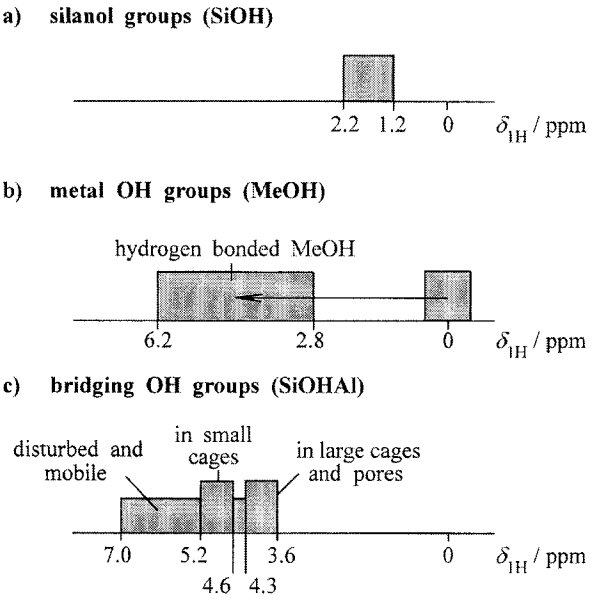


FIG. 4. The ^{1}H NMR shifts of silanol groups in framework defects (a), of metal OH groups at multivalent cations or extra-lattice compounds (b), and of bridging OH groups in different local structures (c).

CaNaY are low-field shifted by $\Delta\delta_{1H}$ = 2.8 ppm with respect to the position of undisturbed MeOH groups (at 0 ppm) due to the formation of hydrogen bonds to neighboring oxygen atoms [17]. An empirical formula describing the interdependence between the O–O distance, d_{OH-O}, of hydrogen bonds responsible for the low-field shift and the value of $\Delta\delta_{1H}$ for hydroxyl groups in inorganic solids was derived by Yesinowski and Eckert [18]:

$$\Delta\delta_{1H}\ (\text{ppm}) = 79.05 - 0.255 d_{OH-O}\ (\text{pm}) \quad (1)$$

According to Eq. (1), the low-field shift of $\Delta\delta_{1H}$ = 2.8 ppm observed for CaOH groups in the sodalite cages of zeolite CaY corresponds to a O–O distance of d_{OH-O} = 0.299 nm. X-ray diffraction (XRD) investigations on dehydrated zeolite CaY yielded extra-framework oxygen atoms with an O–O distance, d_{OH-O}, to the next-nearest framework oxygen atom of 0.297 nm [19]. This value is in reasonable agreement with the O–O distance derived by ^{1}H MAS NMR. In zeolite LaNaY, a low-field shift of the ^{1}H MAS NMR signal of LaOH groups of about $\Delta\delta_{1H}$ = 5.6 ppm was found [9,13]. Depending on the nature of the nonacidic MeOH groups and their location, these hydroxyl protons have ^{1}H NMR chemical shifts in the range 0–6 ppm. In the spectra of dealuminated zeolites HY [9,20], H-mordenite [21] and HZSM-5 [22,23], signals of hydroxyl protons on extra-framework aluminum species appear at chemical shifts in the range 2.6–3.6 ppm. The comparison of these resonance positions with those of AlOH groups on the outer surface of alu-

Downloaded By: [University of Stuttgart] At: 16:06 10 September 2009

minum oxides [24] yields a low-field shift of about $\Delta\delta_{1H} = 3$ ppm. This indicates a formation of hydrogen bonds between the AlOH groups at extra-framework aluminum species and neighboring oxygen atoms. It should also be mentioned that Koller et al. [25] gave evidence for the existence of the low-field-shifted and, therefore, hydrogen-bonded SiOH groups in highly siliceous HZSM-5.

The ^{1}H NMR shifts of bridging OH groups (SiOHAl) cover the range 3.6–7.0 ppm (Fig. 4c). The chemical shift of undisturbed SiOHAl groups in large zeolite cages and pores depend on the framework n_{Si}/n_{Al} ratio [21,26] and, therefore, on the mean electronegativity of the zeolite framework [27]. In Fig. 5, the chemical shift, δ_{1H}, of SiOHAl groups which do not exhibit a hydrogen bond or electrostatic interaction with the zeolite framework [21,27,28] is plotted as a function of the mean Sanderson electronegativity, S^m, of the zeolite frameworks [9]. S^m is defined as the geometric mean of the atomic electronegativities, S_i, so that it follows for zeolites of the composition $H_iAl_jO_kSi_l$ [29]

$$S^m = (S_H^i S_{Al}^j S_O^k S_{Si}^l)^{1/(i+j+k+l)} \quad (2)$$

with $S_{Al} = 2.22$, $S_O = 5.21$, $S_{Si} = 2.84$, and $S_H = 3.55$. The curve shown in Fig. 5 indicates an increase in the chemical shift, δ_{1H}, with increasing mean electronegativity, S^m, of the zeolite framework.

In addition to the above-mentioned signals of undisturbed bridging OH groups, the ^{1}H MAS NMR spectra of zeolites consist of signals due to bridging OH groups influenced by hydrogen bonds or an electrostatic interaction with the zeolite framework. An example is the line at about 4.8 ppm in the ^{1}H MAS NMR spectra of dehydrated zeolites HY due to bridging OH groups pointing into the centers of 6-membered oxygen rings of hexagonal prisms [7,9,21,30,31]. Similar phenomena could be found for other zeolites (e.g., for

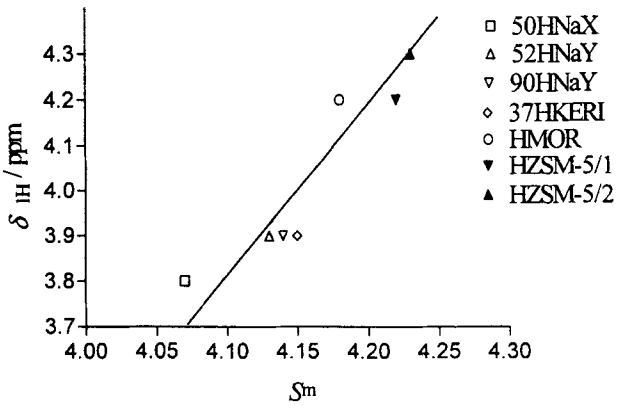


FIG. 5. The ^{1}H NMR shifts δ_{1H} of bridging OH groups in the supercages and channels of zeolites plotted as a function of the mean Sanderson electronegativities, S^m, given in Ref. 9.

Downloaded By: [University of Stuttgart] At: 16:06 10 September 2009

HZSM-5). Applying diffuse reflectance IR spectroscopy, Zholobenko et al. [32] observed a broad band at a position of ~3250 cm^{-1} in the spectrum of zeolites HZSM-5 with n_{Si}/n_{Al} ratios of 21 and 35. This band was explained by acidic OH groups which are hydrogen-bonded to neighboring oxygen atoms (i.e., by bridging hydroxyl group influenced by an additional electrostatic interaction with the zeolite framework).

Experimental data yield a correlation between the chemical shift, δ_{1H}, and the wave number, ν_{OH}, of the IR stretching vibration given by [33]

$$\delta_{1H}\ (\text{ppm}) = 57.1 - 0.0147\nu_{OH}\ (\text{cm}^{-1}) \tag{3}$$

for hydroxyl groups in zeolites and by [33]

$$\delta_{1H}\ (\text{ppm}) = 37.9 - 0.0092\nu_{OH}\ (\text{cm}^{-1}) \tag{4}$$

for hydrogen-bonded protons in various solids. However, the ^1H NMR shifts of MeOH groups bonded to multivalent cations (e.g., to Mg^{2+} or Ca^{2+}) significantly deviate from these correlations. According to Eqs. (3) and (4) the wave number of ~3250 cm^{-1} observed by Zholobenko et al. [32] corresponds to a ^1H MAS NMR signal at resonance positions between 8.0 ppm and 9.3 ppm. Engelhardt et al. [23] first mentioned the existence of a broad shoulder at a chemical shift higher than that of bridging OH groups in HZSM-5 at 4.2 ppm. As it was suggested in Ref. 32, the well-resolved signal at a chemical shift of ~7 ppm observed in the low-temperature ^1H MAS NMR spectrum of zeolites HZSM-5 [34] (see Section VII.B) was ascribed to bridging hydroxyl groups influenced by an additional electrostatic interaction with the zeolite framework [35,36]. The existence of a similar signal could be found for zeolite Beta [37]. A summary of the ^1H NMR shifts of OH groups in dehydrated zeolites is given in Table 1.

B. Residual Linewidth

The full width at half-maximum of the central line of a MAS NMR signal is denoted as the residual linewidth, $\Delta\nu_{1/2}^{MAS}$. The ^1H MAS NMR central line as well as the spinning sidebands may exhibit a characteristic broadening in the presence of a homogeneous interaction such as the homonuclear magnetic dipole–dipole interaction between more than two nuclei (see, e.g., Refs. 44–46). The residual linewidth is then given by

$$\Delta\nu_{1/2}^{MAS} = \frac{1}{A}\frac{(\Delta\nu_{II})^2}{\nu_{rot}} \tag{5}$$

with a $10 \leq A \leq 40$ [45,46]. $\Delta\nu_{II}$ denotes the so-called homonuclear linewidth which can be calculated from the second moment [47]

$$M_2^{II} = \frac{3}{5}\left(\frac{\mu_0}{4\pi}\right)^2 \gamma_I^4\hbar^2 I(I+1)\frac{1}{N_I}\sum_{i\neq j}^{N_I} r_{ij}^{-6} \tag{6}$$

Downloaded By: [University of Stuttgart] At: 16:06 10 September 2009

TABLE 1

^{1}H NMR Shifts and Assignments of Hydroxyl Groups in Dehydrated Zeolites

^{1}H NMR shift δ_{1H} (ppm)	Abbrev.	Type of hydroxyl groups	Ref.
−0.5 . . . 0.5	MeOH	Metal or cation OH groups in large cavities or at the outer surface of particles	17, 39
1.2 . . . 2.2	SiOH	Silanol group at the external surface or at lattice defects	7, 21, 28, 38
2.8 . . . 3.6	AlOH	OH groups bonded to extra-framework aluminum species located in cavities or channels involved in hydrogen bonds	21, 22, 23, 40
2.8 . . . 6.2	CaOH, AlOH, LaOH	Cation OH groups located in sodalite cages of zeolite Y and in channels of ZSM-5 involved in hydrogen bonds	13, 17, 39, 41
3.6 . . . 4.3	SiOHAl, SiO1HAl[a]	Bridging OH groups in large cavities or channels of zeolites	9, 21, 28, 31
4.6 . . . 5.2	SiOHAl, SiO3HAl[a]	Bridging OH groups in small channels and cages of zeolites	9, 21, 28, 31
5.2 . . . 7.0	SiOHAl	Disturbed bridging OH groups in zeolite HZSM-5 and HBeta	8, 27, 34, 36, 42, 43

[a]Assignment of bridging OH groups in faujasite-type zeolites.

Downloaded By: [University of Stuttgart] At: 16:06 10 September 2009

according to [47]

$$\Delta\nu_{1/2} = \frac{1}{\pi}\sqrt{2\ln 2}\sqrt{M_2} \tag{7}$$

for Gaussian lines and with $\Delta\nu_{II} = \Delta\nu_{1/2}$ and $M_2^{II} = M_2$. $\hbar$ denotes Planck's constant h divided by 2π, and μ_0 is the permeability of vacuum. I is the nuclear spin of the resonating nuclei and N_I denotes the number of resonating nuclei in the sample. γ_I is the magnetogyric ratio of the resonating nuclei with spin I and r_{ij} is the internuclear distance. The parameter A depends on the spatial arrangement of the spins and the line shape of the central line [45]. The presence of other line-broadening interactions such as the heteronuclear dipole–dipole interaction and/or the chemical shift anisotropy can lead to a further increase of $\Delta\nu_{1/2}^{MAS}$ [48,49]. The influence of the homonuclear magnetic dipole–dipole interaction upon $\Delta\nu_{1/2}^{MAS}$ can be reduced either by increasing the sample spinning rate, ν_{rot} [see Eq. (5)] or by the application of the so-called CRAMPS technique [50–54]. Furthermore, $\Delta\nu_{1/2}^{MAS}$ is affected by (a) inhomogeneity of the external magnetic field, (b) misadjustment of the magic angle, (c) thermal motions and exchange processes [27,55,26], (d) het-

eronuclear magnetic dipole–dipole interaction with quadrupole nuclei [49,57–60], (e) anisotropy of the magnetic susceptibility [61], and (f) distribution of the isotropic chemical shift [8,49]. If the signals are influenced by inhomogeneous line-broadening effects, the resolution can be improved by increasing the external magnetic field, B_0, because $\Delta\nu_{1/2}^{MAS}$ then strongly depends on ν_0.

The maximum magnetic flux density of the external magnetic fields available on commercial NMR spectrometers presently amounts to 18.8 T. Figure 6 shows ^{1}H MAS NMR spectra of dehydrated zeolites HBeta (a) and HZSM-5 (b), recorded at a resonance frequency of 800.13 MHz with a spinning rate of 12 kHz [43]. The simulation of these spectra leads to the separation of up to seven signals. According to Table 1, the signals at 1.2–2.1 ppm are due to silanol groups. It is interesting to note that there are three types of SiOH groups yielding ^{1}H MAS NMR signals at 1.2 ppm, 1.7 ppm, and 2.1 ppm which can be observed in most of the ^{1}H MAS NMR spectra recorded at B_0 = 18.8 T [43]. For a pure amorphous SiO_2 phase (silica gel), Gay [62] observed a signal of isolated silanol groups at 1.2 ppm. According to Bronnimann et al. [63], SiOH groups in amorphous silica-aluminas cause signals at 1.8–2.1 ppm. Zeolites with low SiOH densities yield signals of isolated silanol groups at a chemical shift of ~1.8 ppm [7,21]. For zeolites

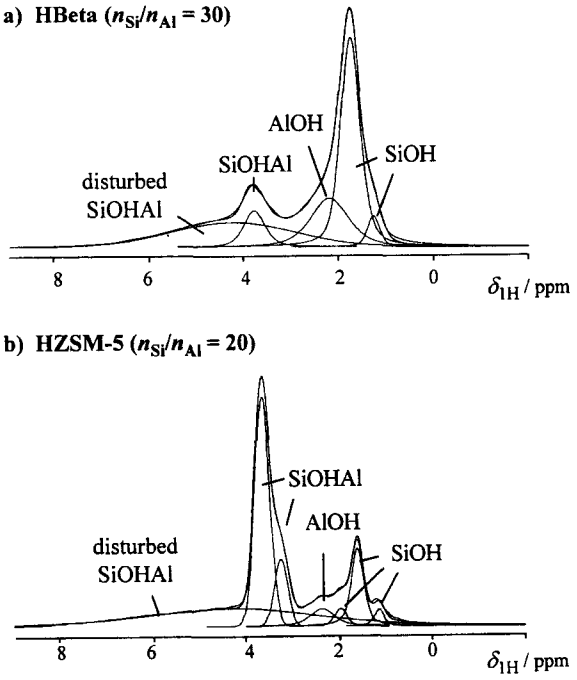


FIG. 6. The ^{1}H MAS NMR spectra of dehydrated zeolites HBeta (a) and HZSM-5 (b), recorded at a resonance frequency of 800.13 MHz with a spinning rate of 12 kHz. (From Ref. 43.)

Downloaded By: [University of Stuttgart] At: 16:06 10 September 2009

with a high SiOH density, signals at ~2.2 ppm were found, probably due to geminal or vicinal SiOH groups (e.g., in zeolite TPA^+/ZSM-5 [22]). Investigating highly siliceous zeolite HZSM-5 ($n_{Si}/n_{Al} > 100$) by IR spectroscopy, Woolery et al. [64] found a broad band at ~3500 cm^{-1} which the authors assigned to *internal silanols* (i.e., to SiOH groups hydrogen-bonded to neighboring framework oxygen atoms). According to Eq. (4), the above-mentioned *internal silanols* cause signals at a chemical shift of ~6 ppm. The ^1H MAS NMR signals at 2.6–3.6 ppm are due to OH groups bonded to extra-framework aluminum species (AlOH). The low-field shift of the signal of these AlOH groups in comparison with the resonance position of the undisturbed AlOH groups at 0 ppm (Table 1) indicates the formation of hydrogen bonds between the hydroxyl protons bonded at extra-framework aluminum species and neighboring oxygen atoms. In agreement with Beck et al. [34,37], the spectral range of bridging OH groups consists of at least two signals. The narrow signal at ~4 ppm has a residual linewidth of $\Delta\nu_{1/2}^{MAS}$ = 300–450 Hz (0.4–0.5 ppm at B_0 = 18.8 T), whereas the broad signal at 4–5 ppm reaches a residual linewidth of $\Delta\nu_{1/2}^{MAS}$ = 2500–3500 Hz. This broad component is caused by bridging OH groups influenced by an additional electrostatic interaction with the zeolite framework (see Section III.A and Table 1). Important to note is the existence of more than one narrow signal with a chemical shift distribution of at least 0.3 ppm [43].

IV. FORMATION OF HYDROXYL GROUPS IN ZEOLITES AND THEIR DEHYDROXYLATION

A. *Formation by Ammonium Exchange*

The most applied method to form bridging OH groups in zeolites is the exchange of charge-compensating cations such as Na^+ by ammonium ions and subsequent thermal treatment. Calcination of the ammonium-exchanged zeolites at temperatures of $T > 573$ K results in a removal of ammonia and the formation of SiOHAl groups. Using IR spectroscopy and neutron diffraction, Ward et al. [65,66], Jirak et al. [67], and Czjzek et al. [68] investigated the occupation of the four crystallographically inequivalent proton sites SiO1Al, SiO2Al, SiO3Al, and SiO4Al in dehydrated zeolites HNaY (Fig. 7). For a zeolite HNaY prepared by the exchange of 95% of the sodium cations by NH_4^+ ions and subsequent calcination, concentrations of 28.6 OH/unit cell for SiO1HAl groups in the supercages and of 24.5 OH/unit cell for SiO2HAl and SiO3HAl groups located in sodalite cages have been found [68]. SiO4HAl groups in the supercages could not be detected. Figure 8 shows the ^1H MAS NMR spectra of dehydrated zeolites HNaY (n_{Si}/n_{Al} = 2.56) with sodium exchange degrees of 36% (36HNaY), 52% (52HNaY), 71% (71HNaY), and 88% (88HNaY). Decomposition of these spectra was carried out using signals of SiOH groups at 1.8 ppm, of SiO1HAl groups at 3.9 ppm,

Downloaded By: [University of Stuttgart] At: 16:06 10 September 2009

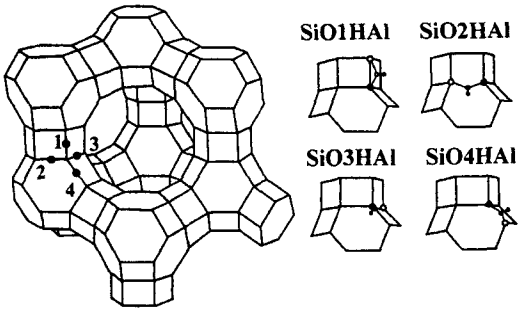


FIG. 7. Structure of zeolite Y with the theoretically possible bridging OH groups at the oxygen atoms O1, O2, O3, and O4. (From Refs. 69 and 70.)

Downloaded By: [University of Stuttgart] At: 16:06 10 September 2009

and of SiO2HAl and SiO3HAl groups at 4.8 ppm. In Fig. 9, the concentrations of SiOHAl groups derived by a quantitative evaluation of the ^{1}H MAS NMR intensities are plotted as a function of the sodium exchange degree. The curves show that exchange degrees of up to 25% of sodium cations cause an exclusive formation of SiOHAl groups at O1 in the supercages of zeolite Y. For exchange degrees larger than 25% of the sodium cations, a linear increase in the concentration of the SiOHAl groups in the sodalite cages (at O2 and O3) could be observed. The ratio between the concentration of bridging hydroxyl groups in the supercages and in the sodalite cages amounts to 0.9 ± 0.1 for a zeolite HNaY with a proton exchange degree of more than 99% [71], which is in agreement with the results of neutron diffraction investigations [68].

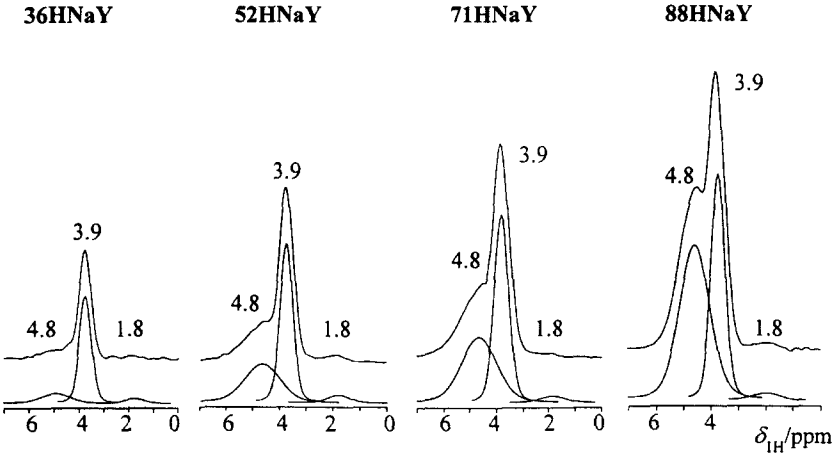


FIG. 8. The ^{1}H MAS NMR spectra of calcined zeolites HNaY ($(n_{Si}/n_{Al} = 2.6)$ after exchange of 36%, 52%, 71%, and 88% of sodium cations by ammonium ions. The spectra were recorded at 400.13 MHz with a spinning rate of 12 kHz. The individual peaks used for the simulation are shown below the spectra. (From Ref. 9.)

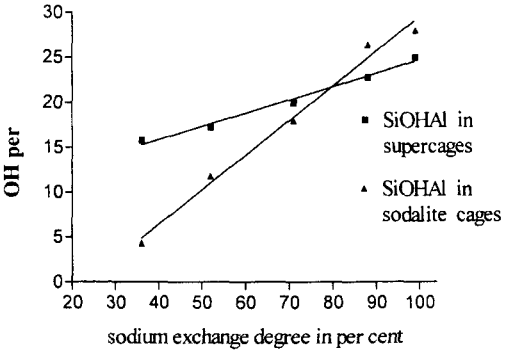


FIG. 9. Concentrations of bridging OH groups in the supercages (signal at 3.9 ppm) and the sodalite cages (signal at 4.8 ppm) of dehydrated zeolites HNaY as function of the degree of sodium exchange. (From Ref. 9.)

Downloaded By: [University of Stuttgart] At: 16:06 10 September 2009

B. Mechanism of Hirschler and Plank

Zeolites exchanged with multivalent cations exhibit strong intracrystalline electric fields. The strength of this potential is proportional to the ratio of the charge and the radius of the cations. According to the mechanism suggested by Hirschler and Plank [72,73], dissociation of water molecules upon adsorption on multivalent cations resulted in the formation of metal OH groups (MeOH) on cations and of bridging OH groups. In Ref. 17, ^{1}H MAS NMR spectroscopy has been applied to investigate quantitatively the formation of hydroxyl protons due to adsorption of water molecules on dehydrated zeolites 83MgNaY and 83CaNaY. The spectra recorded after dehydration at 673 K (Fig. 10, top) only consist of signals due to SiOH groups. Adsorption

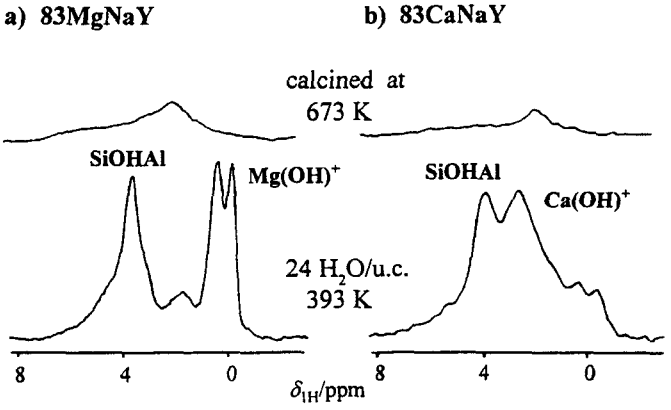


FIG. 10. The ^{1}H MAS NMR spectra of zeolites Y after exchange of 83% of sodium cations with magnesium (a) and calcium (b) and dehydration at T = 673 K (top) and after an additional rehydration with 24 H_2O/unit cell and a second thermal treatment at T = 393 K (bottom). (From Ref. 39.)

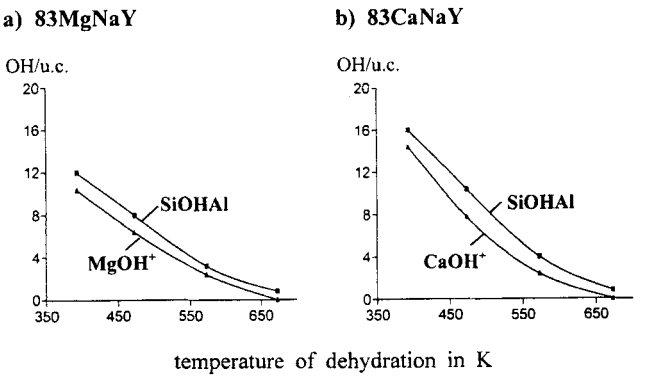


FIG. 11. Concentrations of metal ($MgOH^+$, $CaOH^+$) and bridging OH groups (SiOHAl) formed according to the mechanism of Hirschler and Plank (see text) in zeolites 83MgNaY (a) and 83CaNaY (b) plotted as a function of the dehydration temperature. (From Ref. 39.)

of 24 H_2O/unit cell and a second thermal treatment at 393 K results in signals characteristic for metal ($Mg(OH)^+$, $Ca(OH)^+$) and bridging OH groups (Fig. 10, bottom). An increase of the temperature of the second thermal treatment from 373 to 673 K leads to a significant decrease in the concentrations of MeOH and SiOHAl groups (Fig. 11). The ratio n_{MeOH}/n_{SiOHAl} was found to be about 1:1, which corresponds to a formation of one MeOH group and one SiOHAl group per dissociated water molecule according to the following scheme:

$$2(\equiv Si-O-Al^-\equiv) + Me^{2+} + H_2O \leftrightarrow \equiv Si-O-Al^-\equiv + Me(OH)^+ + \equiv Si-OH-Al\equiv \quad (I)$$

For zeolite LaNaY, a maximum concentration of bridging OH groups occurs after dehydration at T = 523 K [13]. The hydrolysis of aluminum cations was studied on zeolite ZSM-5 exchanged with $Al(NO_3)_3$ [41]. Upon dehydration of zeolite AlZSM-5 at T = 473 K and subsequent water adsorption, a strong increase in the signal of AlOH groups at the chemical shift of 2.8 ppm was found. Dehydration of zeolite AlZSM-5 at temperatures between 473 and 673 K causes a simultaneous decrease of the ^1H MAS NMR signals of AlOH and bridging OH groups [41].

C. *Dehydroxylation and Realumination of Zeolites*

Quantitative multinuclear solid-state NMR investigations of the dehydroxylation of zeolite HY have been published by Freude et al. [74]. Applying ^1H and ^{27}Al MAS NMR spectroscopy, the concentrations of bridging OH groups and tetrahedrally coordinated framework aluminum atoms in a zeolite 88HNaY were determined. Before the measurements, the zeolite was calcined

Downloaded By: [University of Stuttgart] At: 16:06 10 September 2009

at temperatures between 573 and 873 K under shallow and deep bed conditions. In agreement with the dehydroxylation model proposed by Kuehl [75], the decrease in the concentration of the bridging OH groups was found to be equal to the number of tetrahedrally coordinated aluminum atoms removed from the zeolite framework. This result is in contradiction to the dehydroxylation model proposed by Uytterhoeven et al. [76], suggesting that the dehydroxylation of two bridging OH groups leads to the formation of one trigonally coordinated framework aluminum atom.

The ^{1}H NMR investigations of hydrothermally dealuminated zeolites HNaY, H-mordenite, and HZSM-5 have been carried out by Lohse et al. [20], Freude et al. [21], and Engelhardt et al. [23], respectively. Using a zeolite HZSM-5 (n_{Si}/n_{Al} = 15), the interdependence between the treatment conditions and the *n*-hexane cracking activity was investigated [40,77]. After a hydrothermal treatment at T = 813 K with a water-vapor pressure of 6.6 kPa, an increase of the reaction rate of *n*-hexane cracking by a factor of 2.7 in comparison with the parent sample was found. This remarkable effect, which has been first observed by Lago et al. [78], was accompanied by a decrease in the ^{1}H MAS NMR signal of bridging OH groups and the appearance of the ^{27}Al MAS NMR signals of octahedrally and tetrahedrally coordinated extra-framework aluminum species at ~0 ppm and 30 ppm, respectively. The enhanced *n*-hexane cracking activity was, therefore, explained by an interaction between Brønsted acid sites and Lewis acid sites, resulting in the formation of sites with an enhanced catalytic activity.

Using the hydrothermally treated zeolite HNaY, the realumination and rehydroxylation of zeolites were studied. The zeolite HNaY was dealuminated at T = 800 K, subsequently treated with an aqueous KOH solution, and ammonium exchanged [79]. The ^{1}H MAS NMR spectrum of the calcined (673 K) sample showed an increase of the signals of bridging OH groups by a factor of about 2 in comparison with the dealuminated zeolite. This effect was explained by the reinsertion of a corresponding number of extra-framework aluminum atoms into the zeolite framework. In agreement with the ^{1}H MAS NMR data, the ^{29}Si MAS NMR spectrum of the KOH-treated sample yielded a decrease in the framework n_{Si}/n_{Al} ratio from 5.1 to 2.9 and a redistribution of framework aluminum atoms in comparison with the parent sample [79]. The same result has been obtained for hydrothermally dealuminated zeolite HZSM-5 treated with an aqueous NaOH solution [80].

V. ACID STRENGTH OF HYDROXYL GROUPS IN CALCINED ZEOLITES

A. *General Remarks*

Because the ^{1}H NMR chemical shift of undisturbed hydroxyl groups correlates with the mean Sanderson electronegativity, S^m, of the zeolite frame-

Downloaded By: [University of Stuttgart] At: 16:06 10 September 2009

work, it was suggested to make use of δ_{1H} as a measure for the strength of gas-phase acidity [7,21,26,27,30]. This suggestion is confirmed by ab initio quantum-chemical calculations [81] which have revealed a linear interdependence between δ_{1H} and the deprotonation energy ΔE_{DP} of hydroxyl groups which are bonded to T atoms (Al, Si, P, or B) whose first coordination sphere consists of oxygen atoms only. This theoretical study results in a slope of the deprotonation energy of $-(84 + 12)$ kJ mol^{-1} ppm^{-1}. Accordingly, the ^{1}H NMR shift distribution of undisturbed bridging OH groups of at least 0.3 ppm found for zeolite HZSM-5 by high-field ^{1}H MAS NMR spectroscopy (see Fig. 6b) corresponds to a distribution of the deprotonation energy of the Brønsted acid sites in this zeolite of ~25 kJ mol^{-1}.

Recently, Ernst et al. [82] and Freude et al. [83] suggested the quadrupole coupling constant (QCC) of OD groups in zeolites as a scale of acid strength. The electric field gradient at the hydroxyl deuterons studied by ^{2}H NMR spectroscopy on deuterated samples describes the charge distribution in the closer spatial environment of OD groups in zeolites. For zeolites HZSM-5, 92HNaY, and 50HNaX, quadrupole coupling constants of 208 kHz, 224 kHz, and 236 kHz, respectively, were found. However, it is well known that both δ_{1H} and the deuterium QCC are strongly influenced by the presence of hydrogen bonds [84,85] and, therefore, the measurement of the acid strength of hydroxyl groups using these NMR parameters is not faultless.

B. Adsorbate-Induced Chemical Shift

A suitable way to study the acid strength of Brønsted acid sites in solids is the application of probe molecules. Adsorption of strongly basic pyridine molecules on dehydrated zeolites is useful in order to distinguish acidic and nonacidic OH groups (Fig. 12) [6,21,22,86]. Pyridinium ions are formed if pyridine interacts with strongly acidic hydroxyl groups. The interaction between nonacidic hydroxyls such as SiOH groups and pyridine leads to the

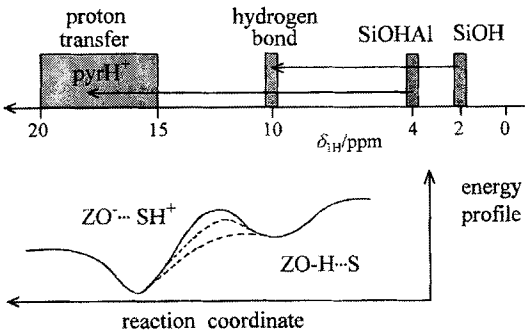


FIG. 12. Adsorbate-induced resonance shifts of the ^{1}H MAS NMR signals of weakly acidic SiOH and strongly acidic SiOHAl groups (top) corresponding to fictive energy profiles of acid–base pairs (bottom).

Downloaded By: [University of Stuttgart] At: 16:06 10 September 2009

formation of hydrogen-bonded complexes. The ^{1}H NMR spectroscopy of organic acids solved in pyridine yields signals of protonated pyridine ($PyrH^+$) at chemical shifts in the range 14–20 ppm [87]. In analogy, the interaction between SiOHAl groups and pyridine in zeolites HNaY [26] and HZSM-5 [86] causes signals at chemical shifts in the range 15.5–19.5 ppm. Simultaneously, the ^{1}H NMR intensity of the acidic OH groups which are involved in this proton-transfer reaction from the zeolite framework to the probe molecules is decreased. In contrast, the interaction of pyridine with SiOH groups in HZSM-5 causes a shift of the ^{1}H MAS NMR signal from 2 ppm to ~10 ppm [86].

In a number of studies on zeolite acidity, the strong base trimethylphosphine (TMP) was used as probe molecule [88–90]. Because the isotope ^{31}P occurs with the natural abundance of 100%, this method does not necessarily require the application of the cross-polarization technique. Lunsford et al. [88] studied TMP adsorbed on zeolite HY by ^{31}P MAS NMR spectroscopy. After adsorption of TMP, the samples under study were degassed at T = 353 K for 30 min to avoid signals of physisorbed probe molecules. For zeolite HY calcined at T = 673 K, the spectrum is dominated by a signal at about −3 ppm (referenced to 85% H_3PO_4) due to $(CH_3)_3PH^+$ complexes arising from chemisorption of TMP at Brønsted acid sites [88]. Zeolites HY calcined at T = 773 K show additional ^{31}P MAS NMR signals in the region from about −32 ppm to −58 ppm due to the chemical interaction of TMP with Lewis acid sites [88]. Hence, TMP is a sensitive NMR probe molecule for Brønsted and Lewis acid sites. However, TMP is rather large and the determination of acid sites in zeolites is, therefore, restricted by the maximum adsorption capacity of the pore system as well as sterical hindrances [89].

Biaglow et al. [91] carried out ^{13}C MAS NMR measurements of ^{13}C(2)-enriched acetone adsorbed on zeolites HZSM-5, HZSM-12, HZSM-22, HY, H-mordenite, SAPO-5, and MeAPO-5. To investigate the slow-exchange range in the presence of adsorbed molecules, the measurements were carried out at T = 125 K. The adsorption of one acetone per bridging OH group leads to a low-field shift of the resonance positions of the C(2) atoms relative to pure acetone between 10.1 ppm for SAPO-5 and 18.7 ppm for HZSM-22. Therefore, the authors suggest that the ^{13}C NMR shift of carbonyl carbon atoms in acetone may be used as a measure of the strength of Brønsted acid sites in zeolites.

Variable-temperature ^{1}H MAS NMR studies of zeolite HZSM-5 loaded with weak bases interacting with zeolitic hydroxyl groups via hydrogen bonds have been reported by White et al. [92], Haw et al. [93], and Brunner et al. [36]. After adsorption of about one probe molecule per bridging OH group on zeolite HZSM-5, adsorbate-induced ^{1}H MAS NMR low-field shifts for ethylene of 2.7 ppm, for carbon monoxide of 1.8 ppm, and for ethane of 0.6 ppm were found at the temperature of T = 123 K [93]. Hence, the adsorbate-induced resonance shift is extremely sensitive to the type of probe molecule used. Koch et al. [94] studied the adsorbate-induced low-field shift of the ^{1}H

Downloaded By: [University of Stuttgart] At: 16:06 10 September 2009

MAS NMR signal of bridging OH groups as a function of the temperature. For zeolite HZSM-5 loaded with one molecule carbon monoxide per bridging OH group, a low-field shift of $\Delta\delta_{1H} = 2.0$ ppm was observed at $T = 123$ K. In this case, the adsorbate-induced wave-number shift of the IR stretching vibration of bridging OH groups amount to $\Delta\nu = 300$ cm^{-1} [94]. From the linear correlation between the IR wave numbers and ^{1}H NMR shifts of hydrogen-bonded hydroxyl protons [Eq. (4)], a corresponding low-field NMR shift of $\Delta\delta_{1H} = 2.8$ ppm follows. This indicates that for adsorption of CO even at $T = 123$ K, the influence of thermal motions on the ^{1}H resonance position of the adsorbate complex is not completely removed.

The interaction of hydroxyl groups in zeolites with perchloroethylene has been investigated by Sachsenroeder et al. [95]. Figure 13 shows the ^{1}H MAS NMR spectra of a dehydrated zeolite HZSM-5 ($n_{Si}/n_{Al} = 17$) recorded at $T = 130$ K before and after adsorption of 2 C_2Cl_4/unit cell and 12 C_2Cl_4/unit cell. In the beginning of the 1980s, Paukshtis and Yurchenko [96,97] developed a method which allows the determination of the deprotonation energy, ΔE_{DP}, of hydroxyl groups in solids by their adsorbate-induced IR wave-number shifts, $\Delta\nu$. Because of the linear correlation between $\Delta\delta_{1H}$ and $\Delta\nu$, the adsorbate-induced ^{1}H MAS NMR low-field shift, $\Delta\delta_{1H}$, can also be used to calculate the deprotonation energy, ΔE_{DP}, of SiOHAl groups contributing to weakly hydrogen-bonded complexes [95]:

$$\Delta E_{DP}\ (\text{kJ mol}^{-1}) = -\frac{1}{C}\log\frac{|\Delta\delta_{1H,SiOHAl}|}{|\Delta\delta_{1H,SiOH}|} \tag{8}$$

with $C = 0.00226$ [96] and the ^{1}H MAS NMR low-field shifts $\Delta\delta_{1H,SiOH}$ and $\Delta\delta_{1H,SiOHAl}$ induced by the adsorbate molecule for the resonance positions of

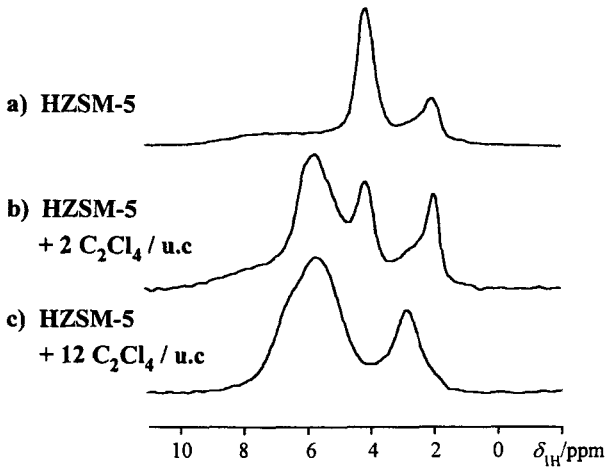


FIG. 13. The ^{1}H MAS NMR spectra of zeolite HZSM-5 recorded at $T = 130$ K before (a) and after adsorption of 2 C_2Cl_4/unit cell (b) and 12 C_2Cl_4/unit cell (c). (From Ref. 95.)

Downloaded By: [University of Stuttgart] At: 16:06 10 September 2009

silanol and bridging OH groups, respectively. With $\Delta\delta_{1H,SiOH} = 0.75$ ppm and $\Delta\delta_{1H,SiOHAl} = 1.9$ ppm observed after adsorption of 12 C_2Cl_4/unit cell on dehydrated zeolite HZSM-5 (Fig. 13c), a deprotonation energy of the SiOHAl groups in the zeolite HZSM-5 of $\Delta E_{DP} = -179$ kJ mol^{-1} follows. With the same method, a deprotonation energy of $\Delta E_{DP} = -146 \pm 30$ kJ mol^{-1} was found for bridging OH groups in the supercages of a dehydrated zeolite 30HNaY [95].

VI. ACCESSIBILITY AND LOCATION OF HYDROXYL GROUPS IN ZEOLITES

A. Application of Probe Molecules

The location of hydroxyl groups in zeolites can be proven upon their interaction with suitable probe molecules. These probe molecules may be strong, medium, or weak bases such as pyridine, ammonia, and even benzene, light paraffines, or fluorinated compounds. Adsorption of deuterated cyclohexane (kinetic diameter: 0.6 nm [69]) on dehydrated silicoaluminophosphate SAPO-5, for example, leads to a significant decrease of the ^{1}H NMR signal of bridging OH groups at 3.8 ppm which is explained by a H–D exchange between probe molecules and hydroxyl protons, indicating a location of the corresponding hydroxyl protons in 12-ring pores [98] (free diameter: 0.73 nm [69]). After adsorption of pyridine on dehydrated silicoaluminophosphate SAPO-34, no change in the signal or bridging OH groups at 3.8 ppm was observed [98]. In this case, the pyridine molecules cannot enter the 8-ring windows of the chabazite cages (free diameter: 0.38 nm [99]). However, ammoniation of dehydrated SAPO-34 gives rise to a ^{1}H MAS NMR signal of ammonium ions at 6.5 ppm [98] which indicates an accessibility of the bridging OH groups in this chabazite-like silicoaluminophosphate for molecules with a size of 0.26 nm (kinetic diameter of ammonia [69]).

As an example, Figure 14 shows the ^{1}H MAS NMR spectra of a dehydrated (673 K) zeolite 88HNaY recorded during in situ adsorption of perdeuterated pyridine (C_5ND_5) with a partial pressure of 1.1×10^3 Pa within 2 h. The spectrum on top corresponds to the unloaded zeolite 88HNaY and consists of signals at 1.8 ppm, 3.9 ppm, and 4.8 ppm due to SiOH groups at framework defects and SiOHAl groups in supercages and sodalite cages (compare Fig. 8). The weak signal at 6.8 ppm is attributed to residual ammonium ions [9]. The strong MAS sidebands are caused by the low sample spinning rate. With increasing adsorption time (from top to bottom) the signal of bridging OH groups in the supercages at 3.9 ppm decreases while all other signals are nearly unaffected by the probe molecules. This behavior indicates that acidic OH groups located in supercages are preferred adsorption sites for the basic probe molecules and that SiOHAl groups located in the sodalite cages are not accessible for pyridine.

Downloaded By: [University of Stuttgart] At: 16:06 10 September 2009

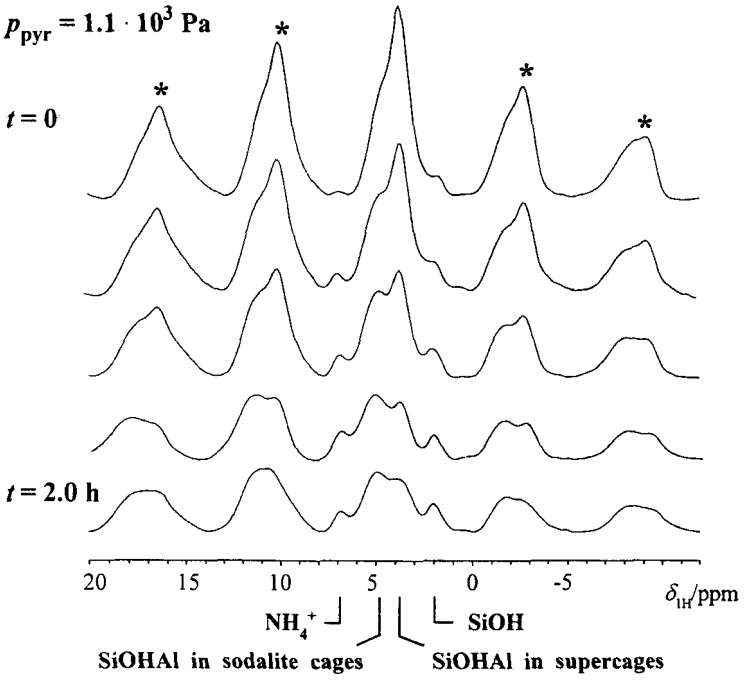


FIG. 14. The ^{1}H MAS NMR spectra of dehydrated (673 K) zeolite 88HNaY recorded at a resonance frequency of 400.13 MHz with a sample spinning rate of ν_{rot} = 3 kHz and during in situ adsorption of perdeuterated pyridine (C_5ND_5) with a partial pressure of 1.1 × 10^3 Pa (*: spinning sidebands). (From Ref. 100.)

B. Sophisticated Pulse Experiments

The direct dipolar interactions between hydroxyl protons and neighboring nuclei open an additional method to investigate the location of OH groups in zeolites. The intensity of ^{29}Si MAS NMR signals of silicon atoms, which are dipolar-coupled with protons in their closer spatial environment, can be enhanced by application of the cross-polarization (CP) technique. The principle of this technique is demonstrated in Fig. 15a. The experiment starts with a $\pi/2$ pulse applied to the ^{1}H nuclei (spin I). Spin polarization is transferred from the ^{1}H nuclei to the ^{29}Si nuclei (spin S) during the application of a contact pulse if the condition ($I = S = 1/2$)

$$\gamma_S B_{1S} = \gamma_I B_{1I} \tag{9}$$

is fulfilled [101]. Equation (9) is called the Hartmann–Hahn condition [102]. B_{1I} and B_{1S} denote the magnetic field amplitudes of the radio-frequency pulses applied to the I and S spins, respectively. A free-induction decay can be observed for the S spins after the contact pulse. The application of this technique allows the selective investigation of $(TO)_3SiOH$ and $(TO)_2Si(OH)_2$ groups, giving rise to signals at ~ −100 ppm and −90 ppm, respectively

Downloaded By: [University of Stuttgart] At: 16:06 10 September 2009

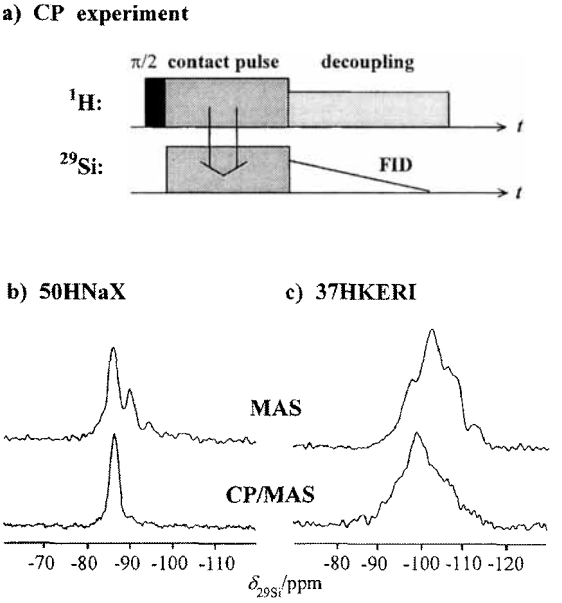


FIG. 15. Schematic representation of the CP experiment (a) and ^{29}Si MAS spectra of dehydrated (673 K) zeolites 50HNaX (b) and 37HKERI (c) recorded without (top) and with (bottom) application of the CP technique. (From Ref. 28.)

[103]. Using dehydrated zeolites, the number of aluminum atoms in the second coordination sphere of the framework silicon atoms, contributing to the local structure of SiOHAl groups, can be determined. In the ^{29}Si CP/MAS NMR spectra of dehydrated zeolite 50HNaX (n_{Si}/n_{Al} = 1.4), for example, only the Si(4Al) signal is enhanced, whereas the lines due to Si(3Al) and Si(2Al) are absent [28] (Fig. 15b). For dehydrated zeolite 37HKERI (n_{Si}/n_{Al} = 2.9), which has two crystallographically inequivalent sites T1 and T2, the signal due to Si_{T1}(2Al) and Si_{T2}(3Al) is enhanced [28] (Fig. 15c). This demonstrates that bridging OH groups in zeolite X and erionite are preferentially bonded to oxygen atoms forming bridges to silicon atoms with a maximum number of framework aluminum atoms in the surrounding.

In recent solid-state NMR investigations, Beck et al. [34,37] applied a dipolar-dephasing spin-echo ^{1}H MAS NMR sequence to zeolites HZSM-5 and HBeta in order to distinguish signals of hydroxyl protons with and without aluminum nuclei in this closer spatial environment. Using the same technique, Freude [42] recorded the ^{1}H dipolar-dephasing spin-echo MAS NMR spectra of a dehydrated HZSM-5 (n_{Si}/n_{Al} = 23). An increase of the length of the dephasing pulses applied to the ^{27}Al spins results in a pronounced decrease of the NMR intensity of the narrow signal at 4.3 ppm and the broad signal at ~7.0 ppm, which shows that both types of hydroxyl groups exhibit a heteronuclear magnetic dipole–dipole interaction with aluminum nuclei.

Often, ^{1}H MAS NMR spectra of dehydrated aluminosilicates and sili-

Downloaded By: [University of Stuttgart] At: 16:06 10 September 2009

coaluminophosphates exhibit signals due to SiOH groups at 1.2–2.2 ppm. For an investigation of the location of these SiOH groups, their homonuclear dipole–dipole interaction with neighboring hydroxyl groups can be exploited by the application of two-dimensional (2D) homonuclear spin diffusion experiments [nuclear Overhauser enhancement and exchange spectroscopy (NOESY)] [104]. The pulse sequence applied for this experiment is depicted in Fig. 16a. The preparation of the spin system with a $\pi/2$ pulse is followed by the evolution period t_1. After the magnetization vector is aligned along the z direction by application of a second $\pi/2$ pulse, spin diffusion takes place between dipolar-coupled hydroxyl protons in the time period Δ. The application of the third $\pi/2$ pulse allows the detection of the magnetization in the x-y plane during the acquisition time t_2. The incrementation of t_1 yields an array, $G(t_1, t_2)$, of free-induction decays which leads, after a twofold Fourier transformation, to the 2D spectrum $F(\nu_1, \nu_2)$.

The ^{1}H MAS NMR spectra of the silicoaluminophosphate SAPO-5 consist of signals at 1.5 ppm due to SiOH groups and at 3.8 ppm and 4.8 ppm caused by bridging OH groups in 12-ring pores and 6-membered oxygen

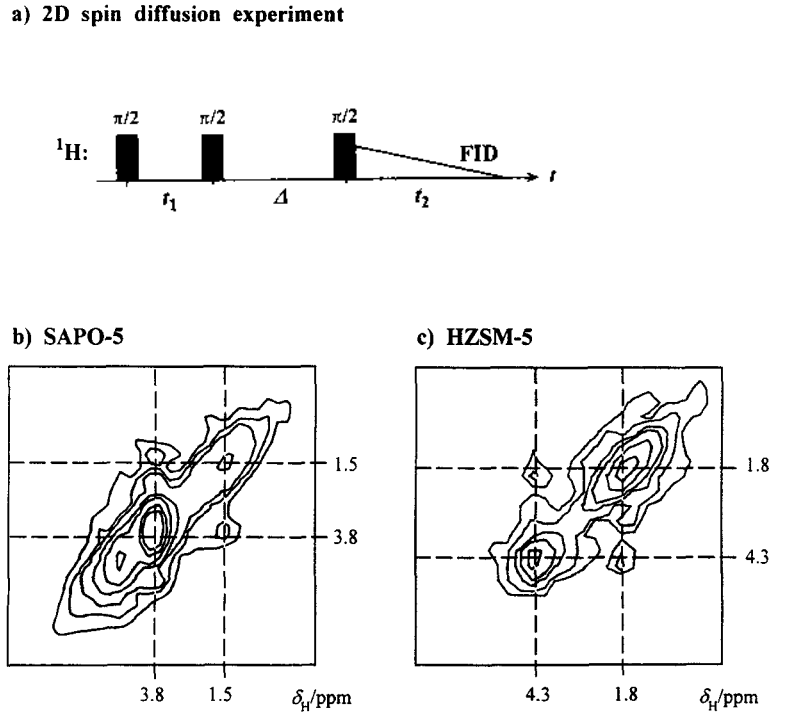
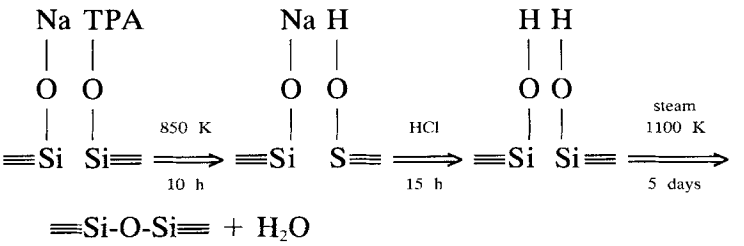


FIG. 16. Schematic representation of the homonuclear 2D spin-diffusion experiment (a) and the contour plots of the 2D ^{1}H NOESY/MAS NMR spectra of hydroxyl groups in the dehydrated silicoaluminophosphate SAPO-5 (b) and the zeolite HZSM-5 (c), recorded at a resonance frequency of 300.13 MHz with a sample spinning rate of 3 kHz and a mixing time of Δ = 50 ms. (From Ref. 9.)

Downloaded By: [University of Stuttgart] At: 16:06 10 September 2009

rings, respectively [28,98,105]. The 2D ^{1}H NOESY/MAS NMR cross-peaks caused by signals at 1.5 ppm and 3.8 ppm (Fig. 16b) indicate a homonuclear dipole–dipole interaction between SiOH groups and bridging OH groups in the 12-ring pores. Hence, most of the SiOH groups must be located in the pores of this crystalline material and not at highly siliceous islands or an amorphous phase.

It is well known that synthesis of ZSM-5 with tetrapropylammonium (TPA^+) iodide or bromide as a structure-directing agent yields zeolite particles with a high concentration of framework defects [38,86]. Up to 8% of the framework silicon atoms in these zeolites are involved in defect SiOH groups. The ^{1}H MAS NMR spectroscopic investigations of zeolite HZSM-5 [38, 106–109], after thermal decomposition of the tetrapropylammonium ions, acid leaching, and steaming, suggested the following scheme (II) for the formation of SiOH in the *as-synthesized* sample:



(II)

This scheme was supported by ^{29}Si CP/MAS NMR and Fourier transform infrared (FTIR) investigations of Woolery et al. [64] and Groenen et al. [110]. The homonuclear 2D ^{1}H NOESY/MAS NMR spectrum of the hydroxyl protons in the dehydrated zeolite HZSM-5 (n_{Si}/n_{Al} = 40) is depicted in Fig. 16c. Cross-peaks due to spin exchange between the signals of SiOH groups at ~2 ppm and bridging OH groups at ~4 ppm indicate a homonuclear dipole–dipole interaction between these hydroxyl protons. Because hydroxyl protons of the bridging OH groups point into the 10-ring pores of zeolite HZSM-5, also most of the silanol groups at framework defects must be located inside the pore of these zeolite particles.

VII. MOBILITY OF HYDROXYL PROTONS

A. Theoretical Description

First investigations of the mobility of hydroxyl protons in H zeolites have been carried out in the 1970s by static ^{1}H NMR spectroscopy [111]. Recent articles have shown that ^{1}H MAS NMR spectroscopy at elevated temperatures also allows the investigation of the proton mobility [9,27,112,113].

At room temperature, the ^{1}H MAS NMR spectra of dehydrated and unloaded zeolites consist of a narrow central line and sharp spinning side-

Downloaded By: [University of Stuttgart] At: 16:06 10 September 2009

bands. Therefore, the correlation time of the hydroxyl protons, τ_c, must be large in comparison with the MAS spinning period $\tau_{rot} = 1/\nu_{rot}$, where ν_{rot} denotes the sample spinning rate. The dominating solid-state interaction of the hydroxyl protons in a SiOHAl group is the dipolar H–Al interaction which results in a line broadening of the statically recorded ^{1}H NMR signal according to Eq. (7) and the second moment defined by [47]

$$M_2^{HAl} = \frac{4}{15}\left(\frac{\mu_0}{4\pi}\right)^2 \gamma_I^2\gamma_S^2\hbar^2 S(S+1)\frac{1}{N_I}\sum_{j=1}^{N_I}\sum_{k=1}^{N_S} r_{jk}^{-6} \tag{10}$$

where the values r_{jk} are internuclear distances, I and S are the nuclear spins of the ^{1}H and ^{27}Al nuclei, N_I and N_S denote the numbers and γ_I and γ_S the magnetogyric ratios of the spins I and S. For hydroxyl protons undergoing uncorrelated statistical jumps with a correlation time, τ_c, the envelope of the free-induction decay is given by [9,27,56,114]

$$G(t) = \exp\left(-\frac{M_2^{HAl}}{3}\left[2J(2\pi\nu_{rot}, t) + J(4\pi\nu_{rot}, t)\right]\right) \tag{11}$$

with

$$\begin{aligned} J(2\pi\nu_{rot}, t) = {} & \frac{t\tau_c}{1 + (2\pi\nu_{rot})^2\tau_c^2} \\ & + \frac{\tau_c^2[(2\pi\nu_{rot})^2\tau_c^2 - 1]}{[1 + (2\pi\nu_{rot})^2\tau_c^2]^2}\left[1 - \exp\left(-\frac{t}{\tau_c}\right)\cos(2\pi\nu_{rot}t)\right] \\ & - \frac{2(2\pi\nu_{rot})\tau_c^3}{[1 + (2\pi\nu_{rot})^2\tau_c^2]^2}\exp\left(-\frac{t}{\tau_c}\right)\sin(2\pi\nu_{rot}t) \end{aligned} \tag{12}$$

Using $4\pi\nu_{rot}$ instead of $2\pi\nu_{rot}$ in Eq. (12) leads to the express of $J(4\pi\nu_{rot}, t)$, which is necessary to calculate $G(t)$. Equation (11) includes several cases which have been discussed in the literature. For the static sample (i.e., for $\nu_{rot} = 0$), Eq. (11) can be transformed in

$$G^{static}(t) = \exp\left\{-M_2^{HAl}\left[\tau_c t + \tau_c^2\exp\left(-\frac{t}{\tau_c}\right) - 1\right]\right\} \tag{13}$$

which corresponds to the model of Anderson and Weiss [115]. For MAS ($\nu_{rot} \neq 0$) and a correlation time $\tau_c \gg t$ (i.e., the rigid lattice), Eq. (11) leads to

$$\begin{aligned} G^{MAS}(t) = \exp\Bigg[& -\left(\frac{M_2^{HAl}}{4\pi^2\nu_{rot}^2}\right) \\ & \times\left(\frac{2}{3}\left[1 - \cos(2\pi\nu_{rot}t)\right] + \frac{1}{12}\left[1 - \cos(4\pi\nu_{rot}t)\right]\right)\Bigg] \end{aligned} \tag{14}$$

Downloaded By: [University of Stuttgart] At: 16:06 10 September 2009

corresponding to the expression published by Schneider et al. [116]. If only the envelope of the free-induction decay is considered, Eq. (11) leads to

$$G^{MAS}(t) = \exp\left[- \left(\frac{M_2^{HAl}}{3}\right)\left(\frac{2\tau_c}{1 + (2\pi\nu_{rot}\tau_c)^2} + \frac{\tau_c}{1 + (4\pi\nu_{rot}\tau_c)^2}\right)\right] \quad (15)$$

Fourier transformation of Eq. (15) yields an expression first published by Andrew and Jasinski [55], which describes the width of the MAS central line as a function of the correlation time, τ_c.

Figure 17 shows the ^{1}H MAS NMR spectra of hydroxyl protons calculated according to Eq. (11) with $M_2^{HAl} = 4.5 \times 10^8$ s^{-2}, $\nu_{rot} = 3$ kHz, and 10 μs $\leq \tau_c \leq$ 10 ms. For $\tau_c = 10$ ms (limiting case of rigid lattice), the MAS sideband pattern consists of narrow lines. In contrast, the lines of the patterns become significantly broader for correlation times in the order of $\tau_{rot} = 1/\nu_{rot}$ and the sidebands disappear. Motional narrowing of the signal can be observed for $\tau_c \ll \tau_{rot}$ because the solid-state interactions are then averaged to zero by isotropic thermal motions. The residual linewidth, $\Delta\nu_{1/2}^{MAS}$, calculated by Eq. (11) for the central line [9,27] agrees well with the results published by Andrew and Jasinski [55]. The residual linewidth of the spinning sidebands, however, significantly exceed this value [9,27].

B. *Experiments*

The ^{1}H MAS NMR spectrum of dehydrated (673 K) HZSM-5 (n_{Si}/n_{Al} = 18) recorded at a temperature of $T = 293$ K exhibit a MAS sideband pattern with a narrow central line at 4.3 ppm [9] (Fig. 18, bottom). Furthermore, a weak signal at 2 ppm due to SiOH groups occurs. The increase of the temperature up to $T = 423$ K (Fig. 18, top) results in a considerable increase of $\Delta\nu_{1/2}^{MAS}$ and a decrease of the relative intensity of the spinning sidebands. A simulation of the spectrum measured at $T = 423$ K using a set of spectra derived by Eq. (11) yields a correlation time of the hydroxyl protons of τ_c = 250 μs [9]. This observation is in agreement with the results published by Sarv et al. [113], who determined for hydroxyl protons in zeolite HZSM-5 a

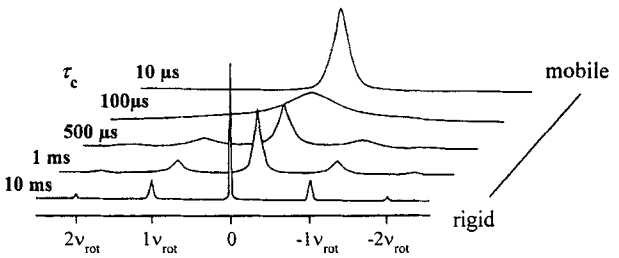


FIG. 17. Proton MAS NMR spectra of hydroxyl protons calculated by Eq. (11) assuming a heteronuclear dipole–dipole interaction corresponding to the second moment of $M_2^{HAl} = 4.5 \times 10^8$ s^{-2}, sample spinning rate of $\nu_{rot} = 3$ kHz, and correlation times, τ_c, given on the left-hand side of the spectra. (From Refs. 9 and 27.)

Downloaded By: [University of Stuttgart] At: 16:06 10 September 2009

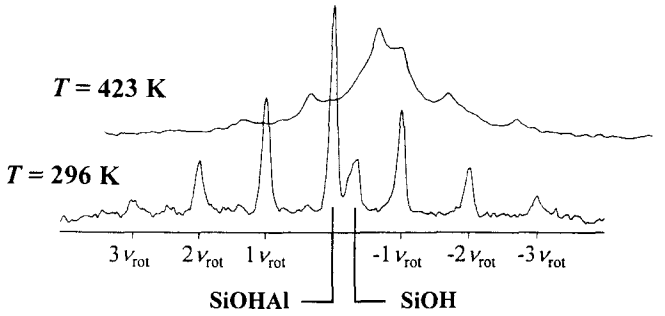


FIG. 18. The ^{1}H MAS NMR spectra of dehydrated (673 K) zeolite HZSM-5 (n_{Si}/n_{Al} = 18) recorded in a stream of nitrogen gas, at the resonance frequency of 400.13 MHz, sample spinning rate of ν_{rot} = 3 kHz, and at temperatures of T = 293 K (bottom) and T = 423 K (top). (From Ref. 9.)

Downloaded By: [University of Stuttgart] At: 16:06 10 September 2009

correlation time of τ_c = 35 μs at T = 500 K and an activation energy of 45 kJ/mol, which corresponds to τ_c = 250 μs at T = 423 K. In Ref. 113, it was furthermore pointed out that the activation energy of ~45–60 kJ mol^{-1} for the thermal motions corresponds to the average proton affinity difference of the four oxygen atoms bonded to the framework aluminum atom. Freude [42] explained that the hydroxyl protons of SiOHAl groups may exchange between at least two of the four oxygen atoms around a framework aluminum atom. At one or more of these positions, the proton exhibits an additional interaction with other framework oxygen atoms. On the other hand, Baba et al. [112] have found a correlation between the framework aluminum concentration and the proton mobility of HZSM-5.

Beck et al. [34] carried out ^{1}H MAS NMR investigations of dehydrated (673 K) zeolite HZSM-5 (n_{Si}/n_{Al} = 19) at low temperatures. Figure 19 shows the spectra recorded in the temperature range 296–123 K. With decreasing temperature, the shoulder at the low-field side of the signal at 4.3 ppm is shifted to the resonance position of 6.9 ppm. By irradiating the aluminum spins during acquisition of the ^{1}H MAS NMR signals, which was called *quadrupole tickling*, Beck et al. [34] proved that the signal at 6.9 ppm corresponds to a novel type of bridging OH groups in zeolite HZSM-5. The large chemical shift of these OH groups can be explained by a hydrogen bond between the hydroxyl protons of SiOHAl groups and neighboring oxygen atoms (i.e., by an additional electrostatic interaction with the zeolite framework). The temperature dependence of the low-field signal indicates a proton exchange between at least two kinds of oxygen atoms around a framework aluminum atom. At one of these oxygen atoms, the proton is influenced by an additional electrostatic interaction (high chemical shift), whereas at the other oxygen atom, no additional electrostatic interaction (low chemical shift) occurs. At low temperatures, this rapid exchange is frozen and the ^{1}H MAS NMR signal due to hydroxyl protons influenced by an additional electrostatic interaction appears as a distinct signal at 6.9 ppm.

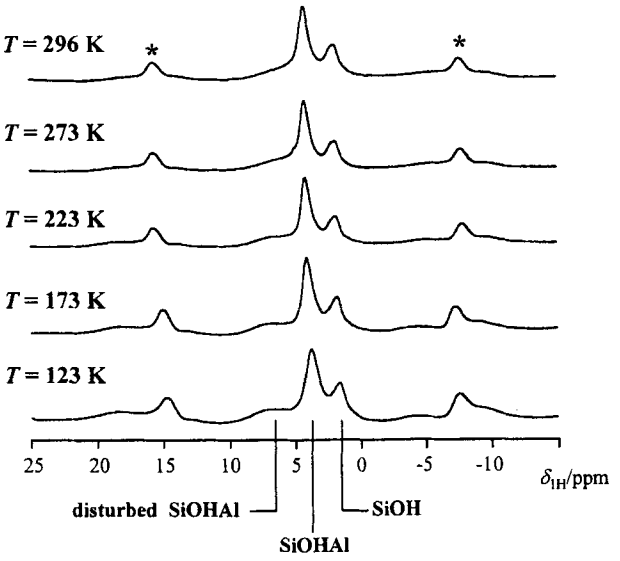


FIG. 19. The ^{1}H MAS NMR spectra of dehydrated (673 K) zeolite HZSM-5 (n_{Si}/n_{Al} = 19) recorded at a resonance frequency of 300 MHz with a sample spinning rate of 3.5 kHz and in the temperature range 296–123 K. (From Ref. 34.)

VIII. LOCAL STRUCTURE OF BRIDGING HYDROXYL GROUPS

A. *Internal H–Al Distance of Bridging OH Groups*

The local structure of bridging OH groups in zeolites has been investigated in numerous quantum-chemical calculations [117–120]. Schroeder et al. [119] suggested local structures with H–Al distances of 0.239 nm and 0.233 nm for SiO1HAl and SiO3HAl groups in zeolite HY, respectively. Stevenson [10] measured the second moment, M_2^{HAl}, of the broad-line ^{1}H NMR signals of bridging OH groups in zeolite HY and determined an H–Al distance of r_{HAl} = 0.238 nm. This value was verified by Freude et al. [121,122] using the same method. Furthermore, a H–Al distance of r_{HAl} = 0.248 nm could be found for bridging OH groups in HZSM-5. Kenaston et al. [123] applied SEDOR (spin-echo double resonance) experiments to determine the H–Al distance of bridging OH groups in HZSM-5 and obtained a H–Al distance of r_{HAl} = 0.243 nm.

In a new approach, the heteronuclear magnetic dipole–dipole interaction between the protons and the aluminum nuclei within the SiOHAl groups and the chemical shift anisotropy have been derived by an analysis of the spinning sideband patterns of the ^{1}H MAS NMR signals [27,28,124,125]. An important advantage of this method is that the spinning sideband patterns of different signals can be analyzed separately. This means that the NMR parameters can be determined selectively; for example, for bridging OH groups located in

Downloaded By: [University of Stuttgart] At: 16:06 10 September 2009

the 6- and the 12-membered oxygen rings occurring in zeolites HY, SAPO-5, and SAPO-37 [27,28,124].

The spinning sideband patterns of signals at different isotropic chemical shifts can be separated by a rotor-synchronized two-dimensional pulse experiment. In this experiment, the time t_1, after the application of a $\pi/2$ pulse to the resonating spins, amounts to multiples of the spinning period $\tau_{rot} = 1/\nu_{rot}$ (i.e., $t_1 = n\tau_{rot}$ with $n = 1, 2, \ldots$). Following the proposal of Aue et al. [126], a π pulse was applied after t_1. Acquisition of the signal as a function of t_2 was started immediately after the π pulse. By this way, the spinning sidebands are removed from the F1 dimension of the two-dimensional spectrum $F(\nu_1, \nu_2)$ (Fig. 20, top), whereas the spinning sideband patterns of the separated signals remain in the F2 dimension (Fig. 20, bottom).

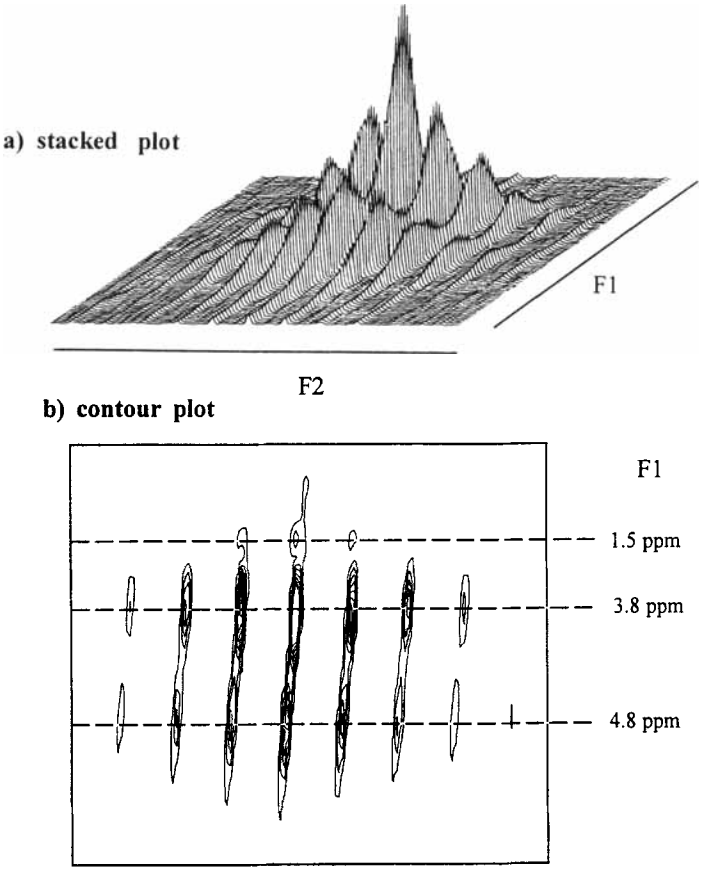


FIG. 20. Stacked plot (top) and contour plot (bottom) of the 2D ^{1}H MAS NMR spectrum of dehydrated (673 K) silicoaluminophosphate SAPO-5. The spectrum was recorded at the proton resonance frequency of 300 MHz with a sample spinning rate of ν_{rot} = 2 kHz and a rotation-synchronized pulse sequence with multiples of $1/\nu_{rot}$ as maximum 64 increments in the period t_1 (see text) to eliminate MAS modulation in the F1 dimension. (From Ref. 9.)

Downloaded By: [University of Stuttgart] At: 16:06 10 September 2009

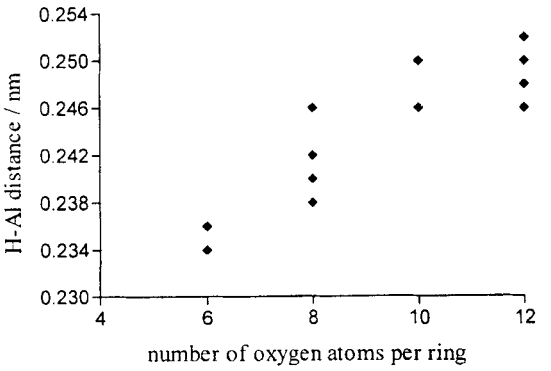


FIG. 21. Plot of the experimentally derived H–Al distances r_{HAl} of bridging OH groups as a function of the number of oxygen atoms per oxygen ring in which the hydroxyl protons are located. (From Refs. 9 and 28.)

Downloaded By: [University of Stuttgart] At: 16:06 10 September 2009

The simulation of the spinning sideband patterns of bridging OH groups was carried out according to the method described in Refs. 28 and 124. The H–Al distances, r_{HAl}, derived by this method are depicted in Fig. 21 as a function of the number of oxygen atoms in the oxygen rings in which the hydroxyl protons are located. The variation of these values suggests that the H–Al distances of bridging OH groups depend on the size of the oxygen rings. A difference of 0.015 ± 0.004 nm between the H–Al distance of SiOHAl groups in the supercages (r_{HAl} = 0.250 ± 0.002 nm) and in the sodalite cages (r_{HAl} = 0.235 ± 0.002 nm) of zeolites HY and SAPO-37 could be found [28,124]. By quantum-chemical investigations, values of r_{HAl} = 0.239 and 0.233 nm were determined for SiO1HAl and SiO3HAl groups, respectively [118,119]. The observation of shorter H–Al distances for SiOHAl groups in the sodalite cages also agrees with the results of neutron diffraction analysis [68,127].

Using the above-mentioned spinning sideband analysis, Koch et al. [94] investigated the influence of carbon monoxide adsorption on the H–Al distance of bridging OH groups in zeolite HZSM-5. For unloaded and loaded (~1 CO/SiOHAl) zeolite HZSM-5, the same H–Al distance was found. However, the chemical shift anisotropy increases significantly from $\Delta\sigma_{OH}$ = 14 ± 2 ppm to $\Delta\sigma_{OH}$ = 22 ± 2 ppm after adsorption of carbon monoxide due to the formation of a linear adsorbate complex. At T = 123 K, an equilibrium distance between the hydroxyl proton and the carbon atom of the probe molecule of r_{HC} = 0.20 ± 0.02 nm could be measured, which is in reasonable agreement with the values derived by quantum-chemical calculations [128–130] and ^{13}C NMR investigations [131].

B. Flexibility of the Local Structure

In a number of studies, multinuclear solid-state NMR spectroscopy has been applied to investigate the variation of the local structure of SiOHAl

groups in dehydrated zeolites due to the protonation or deprotonation of the zeolite framework [9,132–134]. The ^{29}Si MAS NMR spectroscopy of dehydrated NH_4-form and H-form zeolites allows the determination of resonance shifts of Si(*n*Al) signals induced by the protonation of Si–O–Al bridges [132,133]. As demonstrated in Fig. 22, the application of the CP technique enhances selectively the Si(*n*Al) signals of silicon atoms which are coupled with protons of ammonium ions (NH_4-form zeolites) or of hydroxyl groups (H-form zeolites) by dipolar ^{1}H–^{29}Si interactions. According to these spectra, the protonation of Si–O–Al bridges in the result of the deammoniation of the sample leads to a ^{29}Si CP/MAS NMR high-field shift of the Si(1Al) signal (i.e., of those sites which are involved in the local structure of bridging OH groups). For zeolites HMOR and HZSM-5, ^{29}Si CP/MAS NMR high-field shifts amount to 2.7 ppm and 4.0 ppm, respectively [132]. On the other hand, only a high-field shift of 0.8 ppm was observed for zeolite Y/de and no shift was found for zeolite Y [132]. Because of the statistical distribution of aluminum atoms in the zeolite frameworks under study, it is not possible to determine the Si–O–T bond angles in the local structure of bridging OH groups by diffraction methods. However, for zeolites with $n_{Si}/n_{Al} = 1$ (sodalites, zeolite A) and for zeolites built of SiO_4 tetrahedra only (silicalite, dealuminated ZSM-5), the mean Si–O–T bond angles, $\bar{\alpha}$, can be derived by

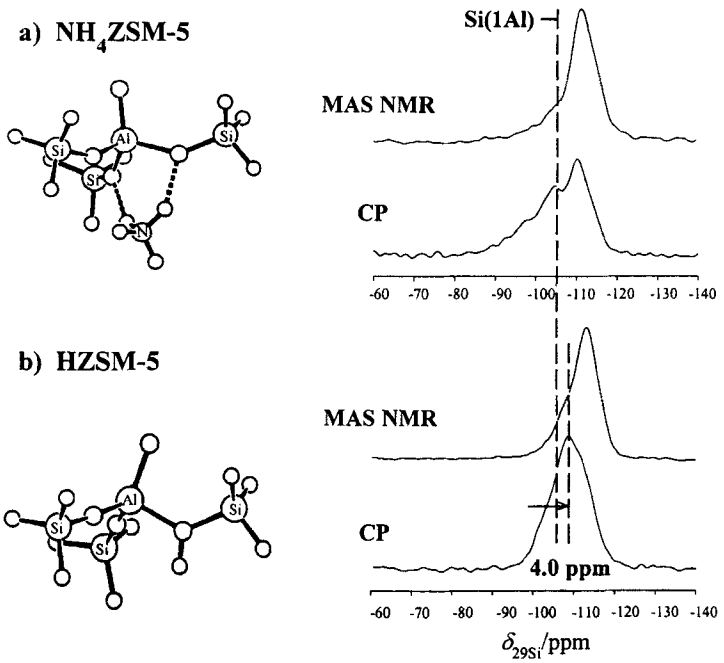


FIG. 22. Scheme of a nonprotonated (left, top) and a protonated (left, bottom) Si–O–Al bridge and the ^{29}Si NMR spectra of these arrangements in dehydrated zeolites NH_4ZSM-5 (right, top) and HZSM-5 (right, bottom) recorded with and without the application of the CP technique. (From Ref. 133.)

Downloaded By: [University of Stuttgart] At: 16:06 10 September 2009

XRD. As known from the literature [135,136], there is a linear relationship between the mean Si–O–T bond angles, $\bar{\alpha}$, determined by XRD and the ^{29}Si MAS NMR shifts of silicon atoms at crystallographically nonequivalent T sites with a slope of −1.7. Applying this slope, the above-mentioned protonation-induced ^{29}Si NMR high-field shifts correspond to a variation of the mean Si–O–T bond angles, $\bar{\alpha}$, in the local structure of bridging OH groups by 1.5° for zeolite Y/de (n_{Si}/n_{Al} = 8.0), 5° for mordenite (n_{Si}/n_{Al} = 8.0), and 7° for zeolite ZSM-5 (n_{Si}/n_{Al} = 22.0) [132,133]. Hence, the Si–O–Al bridges in zeolites respond to the attack of the hydroxyl protons by an increase in the mean bond angles, and this effect is larger for zeolite ZSM-5 than for zeolites MOR and Y. Using the quantitative correlation between the mean Si–O–T bond angles, $\bar{\alpha}$, and the ^{29}Si MAS NMR shift values of Si(nAl) signals (n = 1, 2, 3, 4) published by Radeglia and Engelhardt [137], absolute values of the mean Si–O–T bond angles in the local structure of bridging OH groups in zeolites HY/de, HMOR, and HZSM-5 of about 140°, 151°, and 153°, respectively, can be estimated. This agrees with theoretical investigations [138,139] which yielded a larger mean Si–O–T bond angle in the local structure of SiOHAl groups in zeolites with the stronger Brønsted acid sites.

In dehydrated zeolites, the interaction of the electric quadrupole moment, Q, of framework aluminum atoms with the electric field gradient, V_{zz}, at the aluminum sites is the dominating ^{27}Al solid-state interaction. The strength of the quadrupole interaction is described by the quadrupole coupling constant QCC = eQV_{zz}/h [140]. Figure 23 shows static ^{27}Al spin-echo NMR spectra of a dehydrated zeolite HZSM-5 (n_{Si}/n_{Al} = 22.0), recorded during in situ adsorption of ammonia. Decomposition of the spectrum derived of the

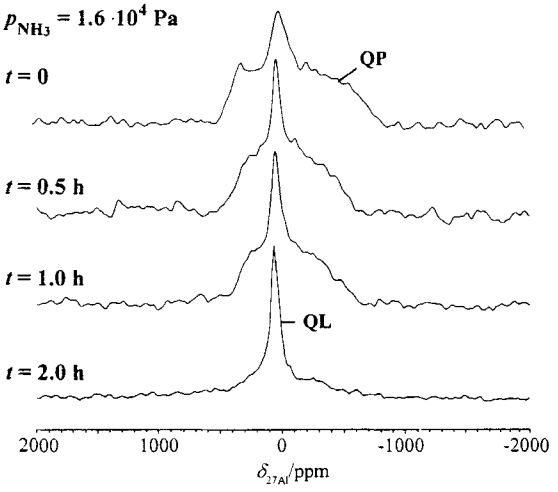


FIG. 23. The ^{27}Al spin-echo NMR spectra of dehydrated (673 K) zeolite 88HNaY recorded at a resonance frequency of 104.2 MHz during in situ adsorption of ammonia (NH_3) with a partial pressure of 1.6 × 10^4 Pa. (From Ref. 100.)

Downloaded By: [University of Stuttgart] At: 16:06 10 September 2009

calcined zeolite HZSM-5 (top) yields two types of signals: a dominating broad quadrupolar pattern (QP) with QCC = 15.5 MHz and a weak quadrupolar line (QL) with QCC of ~7 MHz [133]. The reammoniation of this sample leads to a strong decrease of the signal QP caused by AlO_4 tetrahedra in the protonated zeolite framework (Fig. 23, from top to bottom). After an adsorption time of t = 2.0 h, which corresponds to a complete reammoniation of the dehydrated zeolite HZSM-5, the static ^{27}Al spin-echo NMR spectrum is dominated by the narrow-signal QL (bottom). The structural dependence of the quadrupole coupling constant of AlO_4 tetrahedra in feldspars has been published by Ghose and Tsang [141]. For a quantitative description of the AlO_4 geometry, the authors proposed a *shear–strain parameter* $|\Psi| = \Sigma_i|\tan(\Theta_i - \Theta_0)|$, where the sum runs over the six individual O–Al–O bond angles Θ_i, and Θ_0 is the ideal bond angle of 109.5° [141]. The geometries of AlO_4 tetrahedra given in Refs. 141–143 yield a linear relationship between $|\Psi|$ and QCC. Considering this correlationship, the variation of the aluminum quadrupole coupling constant in the result of the reammoniation of zeolite HZSM-5 (i.e., the deprotonation of the framework) corresponds to an increase in the local symmetry of the framework AlO_4 tetrahedra.

IX. FORMATION OF ADSORBATE COMPLEXES IN ACIDIC ZEOLITES

A. *Adsorption of Methanol on HZSM-5*

Recently, adsorbate complexes formed by methanol molecules bonded on model clusters of bridging OH groups were theoretically investigated by Haase and Sauer [144,145], Gale et al. [146], and Nusterer et al. [147]. These studies suggest that physisorption of methanol on bridging OH groups via two hydrogen bonds is the most stable binding geometry (complex I), whereas a methoxonium cation bonded to the deprotonated fragments (complex II) was found to be a transition state [144,145] (Fig. 24, top). In a number of NMR spectroscopic studies, the chemical interactions of bridging OH groups with probe molecules have been studied [9,132–134,148–150]. Anderson et al. [148] explained the ^1H MAS NMR spectra of zeolite HZSM-5, loaded with more than one methanol molecule per bridging OH group and recorded at room temperature, by a formation of protonated adsorbate complexes. FTIR studies, carried out by Mirth et al. [149], indicated a formation of methoxonium ions in zeolites HZSM-5 also for low methanol coverages. Thursfield and Anderson [150] explained the ^{13}C MAS NMR shifts observed at ambient temperature for low coverages of methanol molecules on zeolite HZSM-5 by rigidly bonded protonated adsorbate complexes. In contrast to these results, ^2H NMR investigations and ^1H spin-echo MAS NMR experiments of adsorbate complexes consisting of one methanol molecule per bridging OH group on zeolite HZSM-5 indicated a high mobility of hydroxyl protons at T = 295

Downloaded By: [University of Stuttgart] At: 16:06 10 September 2009

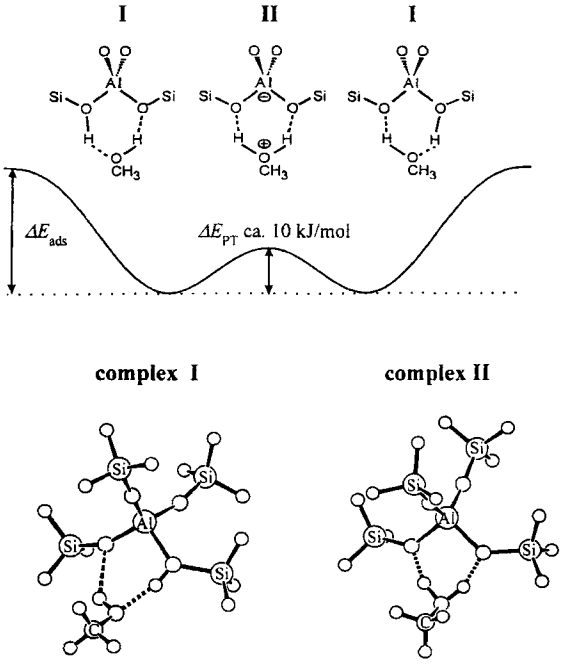


FIG. 24. Adsorbate complexes formed by methanol molecules interacting with model clusters of bridging OH groups derived by quantum-chemical calculations and energy curve for the proton transfer from the SiOHAl group to the adsorbed molecule. In complex I, a methanol molecule is physisorbed via two hydrogen bonds, whereas complex II (ion-pair structure) consists of a methoxonium ion hydrogen bonded at the negatively charged model cluster. (From Ref. 145.)

K [133,134]. Therefore, the experimentally derived ^{1}H NMR shifts are influenced by a rapid chemical exchange of hydroxyl protons between SiOHAl groups and hydrogen-bonded neutral and/or protonated adsorbate complexes [132–134]. In addition, multinuclear solid-state NMR investigations have shown that the adsorption of methanol molecules on zeolite HZSM-5 leads to a variation in the local structure of SiOHAl groups [132–134].

The new injection technique described in Section II.B allows in situ MAS NMR investigations of adsorbate complexes in calcined zeolites. Figure 25 shows the stacked plot of ^{1}H MAS NMR spectra of zeolite HZSM-5 recorded during in situ adsorption of partially deuterated methanol (CD_3OH). The dehydrated zeolite HZSM-5, filled in the in situ MAS rotor, is flushed during the measurements with nitrogen gas which was loaded with CD_3OH (partial pressure of 6.0×10^3 Pa) [134]. The ^{1}H MAS NMR spectra were recorded immediately before ($t = 0$ min) and after ($t > 0$ min) starting the in situ adsorption. The spectrum obtained at $t = 0$ min consists of a signal at 1.8 ppm due to terminal silanol groups and a superposition of two signals at ~4.2 ppm caused by undisturbed bridging OH groups in 10-ring channels (narrow component) and hydrogen-bonded bridging OH groups (broad com-

Downloaded By: [University of Stuttgart] At: 16:06 10 September 2009

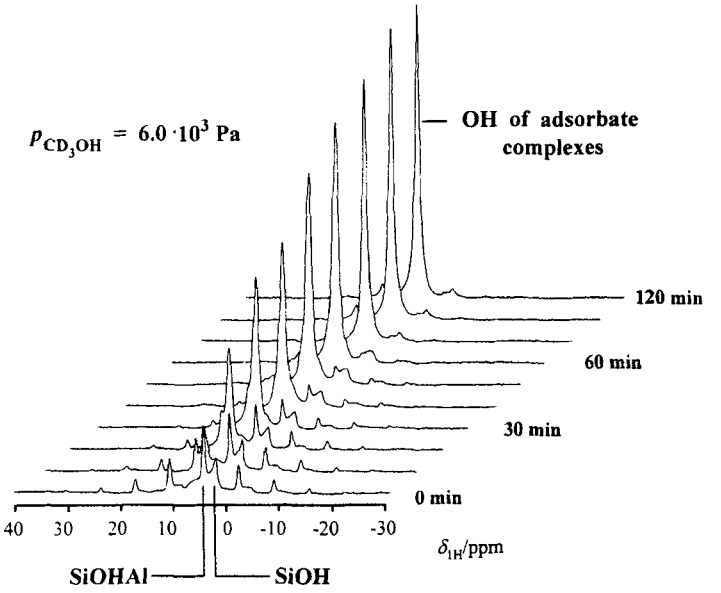


FIG. 25. The ^{1}H MAS NMR spectra of dehydrated zeolite HZSM-5 recorded during in situ adsorption of CD_3OH at T = 295 K. (From Ref. 134.)

ponent, see Table 1). The peaks at ~17 ppm, 11 ppm, −3 ppm, and −9 ppm are due to MAS NMR sidebands (ν_{rot} = 2.5). After starting the adsorption of CD_3OH, a low-field signal appears at ~9 ppm caused by hydroxyl protons of the adsorbate complexes. With running adsorption time, the intensity of the low-field signal increases while the line of bridging OH groups at 4.2 ppm decreases. The fact that the ^{1}H MAS NMR signal of silanol groups remains at the position 1.8 ppm is a hint for the low affinity of these hydroxyl groups to interact with methanol molecules. In Fig. 26, the ^{1}H MAS NMR shifts, δ_{1H}, of the hydroxyl protons involved in adsorption complexes are depicted as a function of the number, n_{CD_3OH}, of the methanol molecules adsorbed per SiOHAl group [134]. Whereas for coverages up to one methanol molecule per SiOHAl group, the ^{1}H MAS NMR shifts are constant at 9.3 ± 0.2 ppm, a further increase of the methanol coverage leads to a decrease of the shift values. Recently, Haase and Sauer [145] published quantum-chemical ab initio calculations on adsorbate complexes formed by one methanol molecule per bridging OH group. The ^{1}H NMR shifts of hydroxyl protons in these model clusters were calculated to 10.8 ppm for the neutral twofold hydrogen-bonded adsorbate complex and to 17.4 ppm for the ion-pair structure. In the ion-pair structure, both hydroxyl protons bonded at the methoxonium ion have the same ^{1}H NMR shift (17.4 ppm) [145]. The ^{1}H NMR shift of the hydroxyl protons in neutral adsorbate complexes of 10.8 ppm is a mean shift value of the hydrogen-bonded hydroxyl protons of the methanol molecule ($CH_3OH\cdots O$: 7.0 ppm) [145] and of the bridging OH

Downloaded By: [University of Stuttgart] At: 16:06 10 September 2009

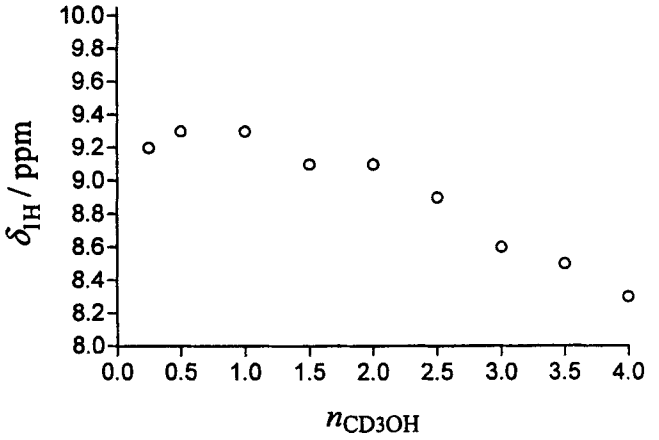


FIG. 26. The ^{1}H MAS NMR shifts, δ_{1H}, of the hydroxyl protons involved in adsorption complexes depicted as a function of the number, n_{CD_3OH}, of molecules per SiOHAl group. (From Ref. 134.) The values n_{CD_3OH} and δ_{1H} were derived by an evaluation of the spectra shown in Fig. 25.

Downloaded By: [University of Stuttgart] At: 16:06 10 September 2009

group (SiAlOH··O: 14.6 ppm) [145]. At room temperature, a rapid chemical exchange occurs between hydroxyl protons of bridging OH groups and of methanol molecules in the physisorbed (complex I in Fig. 24) and/or chemisorbed (complex II in Fig. 24) state. Therefore, the experimentally observed ^{1}H NMR shift of 9–10 ppm agrees very well with the mean shift value of 10.8 ppm, theoretically derived for the neutral twofold hydrogen-bonded complex.

A suitable way to slow down the rapid exchange are measurements at low temperatures. Figure 27 shows ^{1}H MAS NMR spectra of zeolite HZSM-5 loaded with one CD_3OH and one CD_3OD per SiOHAl group and recorded at T = 153 K [134]. Generally, the decrease of the temperature results in a strong broadening of the ^{1}H MAS NMR signals. The existence of MAS sideband patterns indicates that the thermal correlation times, τ_c, of these hydroxyl protons are large in comparison with the period, $\tau_{rot} = 1/\nu_{rot}$, of the MAS frequency, ν_{rot} (see Section VII.A). By a comparison of the spectra of the zeolite HZSM-5 loaded with one CD_3OH/SiOHAl and recorded with MAS frequencies of ν_{rot} = 7.5 kHz (Fig. 27a) and ν_{rot} = 5.2 kHz (Fig. 27b), MAS NMR central lines at 1.8 ppm, 4.1 ppm, 9.6 ppm, and 14.2 ppm can be identified. The signal at 1.8 ppm is due to terminal SiOH groups (see Table 1). The broad signal at ~9.6 ppm corresponds to a residual amount of mobile hydroxyl protons as observed at T = 295 K (compare Fig. 25). The remaining two signals at 4.1 ppm and 14.2 ppm (marked by the dashed line) are due to hydroxyl protons of adsorbate complexes. The splitting of the spectrum into two ^{1}H MAS NMR patterns shows that the transitions between the above-mentioned two symmetry-equivalent adsorbate complexes I (Fig. 24 top) and frozen at T = 153 K. Figure 27c shows the ^{1}H MAS NMR spectrum of zeolite

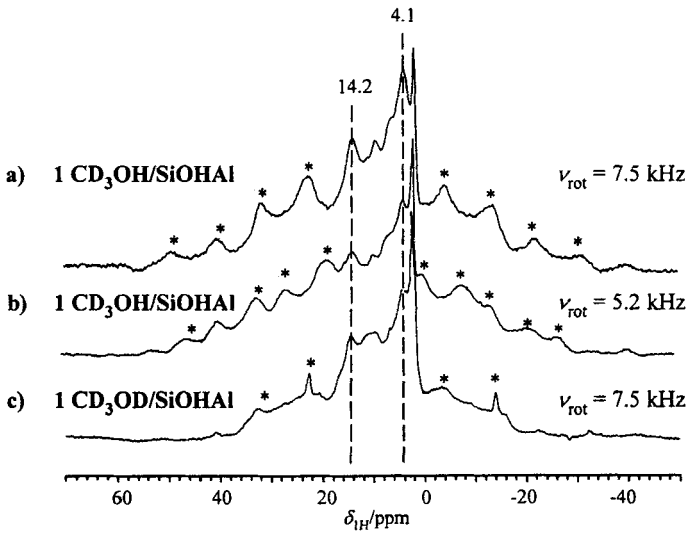


FIG. 27. Low-temperature (T = 153 K) ^{1}H MAS NMR spectra of dehydrated zeolite HZSM-5 loaded with one CD_3OH/SiOHAl (a, b) and one CD_3OD/SiOHAl (c) (*: MAS sidebands). (From Ref. 134.)

HZSM-5 loaded with one CD_3OD/SiOHAl. The fact that also this spectrum consists of two signals at 4.1 ppm and 14.2 ppm indicate a rapid isotopic H/D exchange between the zeolite SiOHAl groups and the methanol OD groups directly after the adsorption of CD_3OD.

B. Influence on the Local SiOHAl Structure

In Section VIII.B is shown the quadrupole coupling constant of framework aluminum atoms in dehydrated zeolites is strongly influenced by adsorption of ammonia. A similar behavior was found for the adsorption of methanol molecules at Brønsted acid sites in dehydrated zeolite HZSM-5. Figure 28 shows the static ^{27}Al spin-echo NMR spectra of a dehydrated zeolite HZSM-5 before (a) and after (b, c) adsorption of methanol, recorded at temperatures of T = 295 K (top) and T = 85 K (bottom) [134]. Decomposition and simulation of the static ^{27}Al spin-echo NMR spectrum of the unloaded zeolite HZSM-5 (Fig. 28a) yield two quadrupolar patterns corresponding to quadrupole coupling constants of QCC = 7.5 ± 0.5 MHz (QP1) and QCC = 15.5 ± 0.5 MHz (QP2). Adsorption of one and three CH_3OH/SiOHAl results in a significant narrowing of the quadrupolar pattern (Figs. 28b and 28c). These spectra consist of only one component which corresponds to a quadrupolar pattern with QCC = 8.0 ± 0.5 MHz (QP3) and to a narrow quadrupolar line with QCC = 2.5 ± 0.5 kHz (QL). Because no variation of the ^{27}Al spin-echo NMR spectra and, therefore, of the ^{27}Al quadrupole coupling constants was found after decreasing the temperature from T = 295 K to T =

Downloaded By: [University of Stuttgart] At: 16:06 10 September 2009

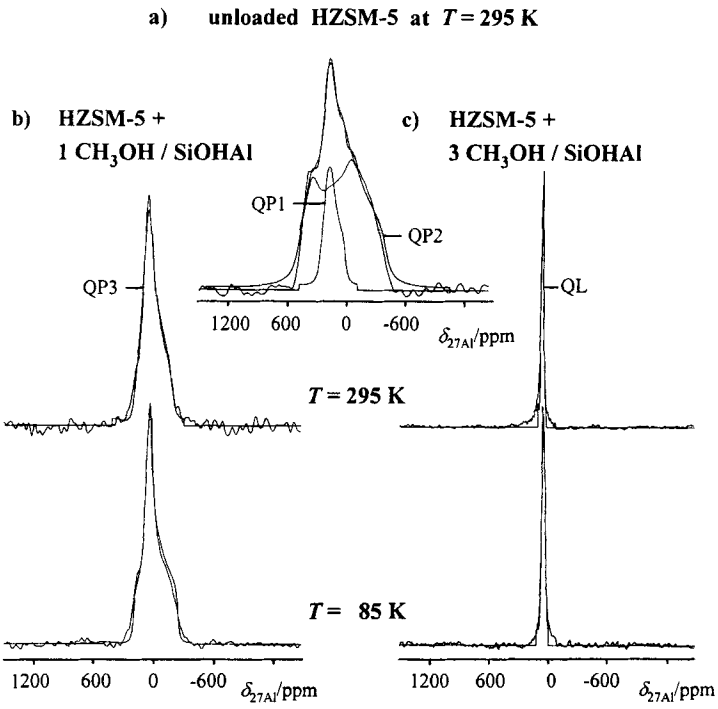


FIG. 28. The ^{27}Al NMR spectra of dehydrated zeolite HZSM-5, unloaded (a) and loaded with one CH_3OH/SiOHAl (b) and three CH_3OH/SiOHAl (c). All samples were recorded with a quadrupole-echo sequence and at temperatures of T = 295 K (b and c, top) and T = 85 K (b and c, bottom). (From Ref. 134.)

85 K, an influence of adsorbate mobility on the ^{27}Al spin-echo NMR line shape can be excluded.

According to the above-mentioned correlation between the ^{27}Al quadrupole coupling constant, QCC, and the local geometry of the AlO_4 tetrahedra in the framework of dehydrated zeolites (Section VIII.B), the decrease of QCC in the result of methanol adsorption from QCC = 15.5 MHz to QCC = 2.5–8.0 MHz corresponds in the first order to a decrease of the *shear strain.* This behavior corresponds to a more symmetric geometry of the AlO_4 tetrahedra. However, a variation of the Al–O bond lengths has to be considered. Ab initio calculations on model clusters of bridging OH groups interacting with methanol [145] and water molecules [151] indicated a change of the O–Al–O bond angles as well as the Al–O bond lengths in the AlO_4 tetrahedra. In both cases, the variation of the O–Al–O bond angles in AlO_4 tetrahedra contributing to the local structure of SiOHAl groups is nearly the same for neutral twofold hydrogen-bonded adsorbate complexes and ion-pair structures [145,151]. On the other hand, there are significant differences in the Al–O bond lengths of the above-mentioned AlO_4 tetrahedra [145,151]. For AlO_4 tetrahedra contributing to ion-pair structures (complex II in Fig.

Downloaded By: [University of Stuttgart] At: 16:06 10 September 2009

24), the Al–O bond length differences are significantly smaller than for AlO_4 tetrahedra of SiOHAl groups contributing to neutral twofold hydrogen-bonded adsorbate complexes [145,151]. This effect may be responsible for the significantly smaller ^{27}Al quadrupole coupling constant of AlO_4 tetrahedra in the local structure of bridging OH groups interacting with three methanol molecules (QCC = 2.5 MHz) in comparison with the QCC value of AlO_4 tetrahedra in the local structure of the SiOHAl groups interacting with one methanol molecule (QCC = 8.0 MHz). Hence, the small ^{27}Al quadrupole coupling constant of framework AlO_4 tetrahedra of zeolite H-ZSM-5 loaded with three methanol molecules per SiOHAl group supports the partial protonation of the adsorbed methanol molecules.

Downloaded By: [University of Stuttgart] At: 16:06 10 September 2009

X. IN SITU INVESTIGATIONS OF REACTIONS CATALYZED BY BRØNSTED ACID SITES

A. General Remarks

In the last decade, in situ NMR spectroscopy has found an increasing application for the investigation of chemical reactions catalyzed by Brønsted acid sites in zeolites. Using this spectroscopic technique, it is possible to study the formation of intermediates and reaction products inside the zeolite crystals and the fate of Brønsted acid sites during the reaction. An excellent review on in situ NMR spectroscopic studies of chemical reactions in zeolites is given by Haw [152]. Furthermore, the reader is referred to articles by Klinowski [153,154], Ivanova and Derouane [155], and Pfeifer and Ernst [156].

Typically, molecules adsorbed on zeolites are characterized by a wide range of thermal correlation times reflecting the differences in their molecular mobilities. Some molecules or species remain in the gas phase or are involved in a rapid exchange with adsorbed molecules. Other species are strongly adsorbed on Brønsted acid sites or are entrapped in small cavities. In addition, the formation of coke results in large immobile complexes. Homonuclear (^1H–^1H) and heteronuclear (^{13}C–^1H) magnetic dipole–dipole interactions of immobile species are the main reasons for a line broadening of ^1H and ^{13}C NMR signals. The mobility of all of these species increases with increasing temperature. In addition, proton decoupling during the acquisition of ^{13}C NMR signals removes residual dipolar ^{13}C–^1H interactions, yielding solution-like conditions. The high mobility of reactant molecules in zeolites and their variation, however, has practical consequences on the application of the CP technique [101]. The inefficiency of the CP technique for mobile compounds makes the corresponding signals less intense than those of rigid species [101] and results in only semiquantitative ^{13}C CP/MAS NMR spectra. On the other hand, CP is advantageous to avoid saturation by long ^{13}C spin-lattice-relaxation times of rigid compounds. The comparison of Bloch decay and CP/MAS NMR spectra is a method suitable for assigning signals [152].

B. Reactions Catalyzed by Acidic Zeolites

In the chemical industry, heterogeneously catalyzed reactions are carried out mostly under continuous-flow conditions. In situ NMR studies of the steady state of these reactions requires the application of a continuous-flow system comparable to that described in Section II.B. With this technique, the fate of the catalytically active Brønsted acid sites can be studied under reaction conditions.

The conversion of alcohols is a well-established reaction for the characterization of acidic catalysts [157,158]. The dehydration of propan-2-ol was studied on zeolites HNaX [159], HNaY [160], and dealuminated HY [161]. The reaction was found to be of first order with respect to adsorbed propan-2-ol and the products were confined to propene, diisopropyl ether, and water. As an example for an in situ MAS NMR investigation under continuous-flow conditions, Fig. 29 shows the ^{13}C MAS NMR spectra recorded during propan-2-ol conversion of zeolite HY [13,14]. The reaction was carried out at a temperature of T = 393 K with a flow of propan-2-ol according to a modified residence time of $W/F_{\text{p-2-ol}}$ = 450 g h/mol [13,14]. Before the investigation, the zeolite was dehydrated in vacuum for 12 h at 673 K. The reactant molecules used in this study were ^{13}C-enriched at the C(2) atom. The NMR spectra recorded after a reaction time of t = 0.5 h consist of a signal at 65–70 ppm due to isotopically enriched C(2) atoms of physisorbed propan-2-ol and/or diisopropyl ether molecules. Additional signals at 10–50 ppm are caused by CH_2 and CH_3 groups of coke precursors, whereas the signal appearing after a reaction time of t = 2.5 h at 220 ppm is due to the formation of acetone. Although propene is one of the main reaction products [13,14], no signal of the C(2) atoms of propene can be observed at 130 ppm. This is caused by the short residence time of the reaction product inside of the MAS NMR microreactor under flow conditions. A variation of the modified resistance time from 450 to 140 g h/mol leads to a strong increase of the signal at 65–70 ppm. This behavior agreees with the above-mentioned assignment of this signal because an increase in the educt flow should result in an increase of the signal of physisorbed educt molecules. After purging the sample with dry nitrogen gas (bottom), this signal is completely removed. As expected, the purging of the sample with dry nitrogen gas leads to no change in the signals of coke precursors at 10–15 ppm. Because the signal of acetone is decreased only by a factor of maximum 2, these molecules must be strongly adsorbed on the zeolite surface, which renders its detection by chromatographic methods difficult.

To study the fate of the catalytically active Brønsted acid sites, ^{1}H MAS NMR spectra of zeolite HY were recorded before (t = 0) starting the propan-2-ol conversion (Fig. 30, bottom) and after a reaction time of t = 15 min (Fig. 30, top) [14]. The spectrum of the zeolite HY recorded at t = 0 consists of the signal of bridging OH groups at 4 ppm with characteristic MAS NMR sidebands marked by asterisks. After the reaction time of t = 15 min, the

Downloaded By: [University of Stuttgart] At: 16:06 10 September 2009

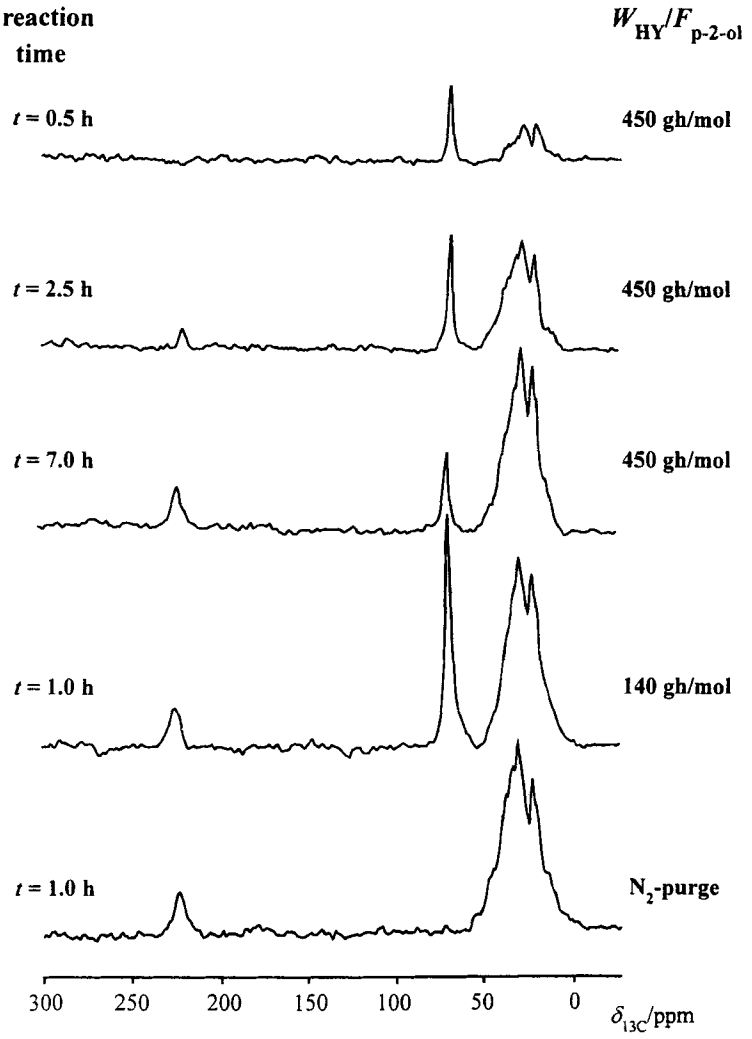


FIG. 29. In situ ^{13}C MAS NMR spectra of zeolite HY recorded at the temperature of T = 393 K under a continuous flow of propan-2-ol with a modified residence time of $W/F_{p\text{-}2\text{-}ol}$ = 450 g h/mol and after reaction times between 0.5 h and 7.0 h (top three). The two spectra shown on the bottom were recorded at T = 393 K under an educt flow corresponding to $W/F_{p\text{-}2\text{-}ol}$ = 140 g h/mol and after purging the sample with dry nitrogen gas for 1 h. (From Refs. 13 and 14.)

signal at ~4 ppm as well as the MAS NMR sideband pattern are strongly decreased. At this reaction time, the spectrum consists of two narrow signals at 1.6 ppm and ~5 ppm, which are due to CH_3 and CH groups of propan-2-ol and/or diisopropyl ether. In the low-field range, an additional broad signal appears at ~8 ppm. Because this signal has no sideband pattern, it should be caused by mobile protons. According to previous ^1H MAS NMR investigations [162,163] and ab initio calculations [151], the adsorption of water mol-

Downloaded By: [University of Stuttgart] At: 16:06 10 September 2009

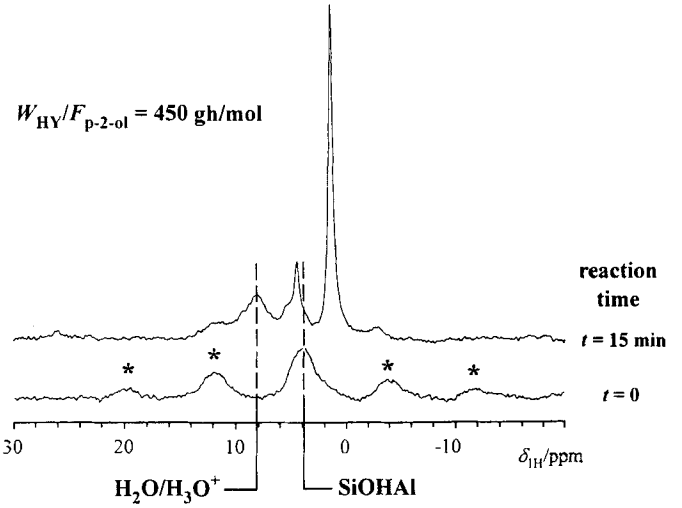


FIG. 30. In situ ^1H MAS NMR spectra of zeolite HY recorded at the temperature of T = 373 K under a flow of dry nitrogen gas (bottom) and after 15 min under a continuous flow of propan-2-ol with a modified residence time of $W/F_{p\text{-}2\text{-}ol}$ = 450 g h/mol (top). (From Ref. 14.)

ecules on bridging OH groups results in a significant low-field shift of the resonance position of all hydroxyl protons. For coverages of more than one water molecule per SiOHAl group, the formation of hydroxonium ions was found [151]. The reaction under study forms water molecules by the dehydration of propan-2-ol. Therefore, the spectrum shown in Fig. 30 (top) indicates a hydration of acidic bridging OH groups in the first 15 min of the propan-2-ol conversion. During this time, the physisorption of water molecules on the bridging OH groups and the formation of hydroxonium ions lead to the broad signal at ~8 ppm while the signal of the free SiOHAl groups at 4 ppm is strongly decreased.

The experiments described above demonstrate that in situ MAS NMR spectroscopy under continuous-flow conditions is an interesting method to investigate compounds with long residence times on surface sites in the pores of zeolites. This method is useful to investigate the initial steps of reactions catalyzed by Brønsted acid sites, the fate of these catalytically active hydroxyl groups, and the formation of by-products and coke precursors in the zeolite pores.

XI. CONCLUDING REMARKS

Solid-state NMR spectroscopic techniques have found numerous applications for the determination of the (a) types of hydroxyl groups in zeolites, (b) their concentration, and (c) accessibility, and for the characterization of the (d) acid strength and (e) local structure. NMR spectroscopy allows the

Downloaded By: [University of Stuttgart] At: 16:06 10 September 2009

study of the (f) mobility of hydroxyl protons and their role in (g) the formation of adsorbate complexes and in (h) heterogeneously catalyzed reactions. Therefore, this spectroscopic method meanwhile belongs to the most powerful techniques for the characterization of Brønsted acid sites in zeolites and related materials. The basis of this success was the invention of new sample preparation techniques, high external magnetic fields, effective line-narrowing methods, and two-dimensional experiments which make the detection of highly resolved solid-state NMR spectra and the separation of different spectral parameters possible.

NOTATION

$\bar{\alpha}$	Mean Si–O–T bond angle
A	Linewidth parameter of Eq. (5)
B_0	Flux density of the external magnetic field, in T
B_{1I}, B_{1S}	Magnetic field amplitudes of radio-frequency pulses applied to the spins I and S
C	Parameter in Eq. (8)
δ_{1H}	Isotropic chemical shift of the ^{1}H NMR spectroscopy, in ppm
d_{OH-O}	O–O distance within hydrogen bonds
Δ	Mixing time in the NOESY experiment
$\Delta\delta_{1H}$	Low-field shift of the ^{1}H NMR spectroscopy, in ppm
ΔE_{DP}	Deprotonation energy, in kJ mol^{-1}
$\Delta\nu$	Adsorbate-induced wave-number shift
$\Delta\nu_{1/2}^{MAS}$	Residual MAS NMR linewidth, in Hz
$\Delta\nu_{II}$	Static linewidth caused by homonuclear dipole–dipole interaction
$\Delta\sigma_{OH}$	Chemical shift anisotropy of hydroxyl protons
ΔT	Temperature gradient, in K
Ψ	Shear-strain parameter
F1	Frequency domain 1 of a two-dimensional spectrum
F2	Frequency domain 2 of a two-dimensional spectrum
γ_I, γ_S	Magnetogyric ratio of nuclei with spin I and S
$G(t)$	Envelope of the free-induction decay
$\hbar$	Planck's constant h divided by 2π
I	Nuclear spin I
μ_0	Permeability of vacuum
M_2^{HAl}	Second moment of the dipolar H–Al interaction, in s^{-2}
M_2^{II}	Second moment of the homonuclear dipole–dipole interaction, in s^{-2}
n_{CD_3OH}	Number of CD_3OH molecules per SiOHAl group
N_I	Number of nuclei with spin I in the sample
ν_{OH}	Wave number of the OH stretching vibration, in cm^{-1}

Downloaded By: [University of Stuttgart] At: 16:06 10 September 2009

ν_{rot}	Sample spinning frequency, in Hz
Q	Electric quadrupole moment, in 10^{-24} cm^2
r_{HAl}	H–Al distance
r_{ij}	Distance of atoms i and j
S_i	Sanderson electronegativity of atom i
S^m	Mean Sanderson electronegativity
Θ_i	Individual O–Al–O angles of an AlO_4 tetrahedron
Θ_0	Ideal O–Al–O angle of a AlO_4 tetrahedron (109.5°)
T	Absolute temperature, in K
τ_c	Correlation time of thermal mobility, in ms
τ_{rot}	Period of sample spinning, in ms
V_{zz}	z Component of the electric field gradient
W/F	Modified residence time, in g h mol^{-1}

Downloaded By: [University of Stuttgart] At: 16:06 10 September 2009

ACKNOWLEDGMENTS

The author gratefully acknowledges the Deutsche Forschungsgemeinschaft, the Max-Buchner-Forschungsstiftung, and the Fonds der Chemischen Industrie for support. Furthermore, the author is indebted to Prof. J. Weitkamp (Institute of Chemical Technology I, University of Stuttgart, Germany) for enabling most of the above-mentioned investigations in the NMR laboratory of his institute.

REFERENCES

1. J. A. Rabo, *Zeolite Chemistry and Catalysis*, ACS Monography 171, American Chemical Society, Washington, DC, 1976.
2. J. A. Rabo and G. J. Gajda, *Catal. Rev.—Sci. Eng.*, *31*, 385 (1989–1990).
3. P. B. Venuto and E. T. Habib, *Fluid Catalytic Cracking with Zeolite Catalysts*, Marcel Dekker, Inc., New York, 1978.
4. P. B. Venuto, *Microporous Mater.*, *2*, 297 (1994).
5. N. Y. Chen, W. E. Garwood, and F. G. Dwyer, *Selective Catalysis in Industrial Applications*, Marcel Dekker, Inc., New York, 1989.
6. D. Freude, M. Hunger, and H. Pfeifer, *Chem. Phys. Lett.*, *91*, 307 (1982).
7. H. Pfeifer, D. Freude, and M. Hunger, *Zeolites*, *5*, 274 (1985).
8. E. Brunner, *J. Mol. Struct.*, *355*, 61 (1995).
9. M. Hunger, *Solid State Nucl. Magn. Reson.*, *6*, 1 (1996).
10. R. L. Stevenson, *J. Catal.*, *21*, 113 (1971).
11. Pyrex glass inserts DWGSK-2576-1 and -2, WILMAD Glass Company, Route 40 and Oak Road, Buena, NJ.
12. M. Hunger and T. Horvath, *J. Chem. Soc., Chem. Commun.* 1423 (1995).
13. M. Hunger, T. Horvath, and J. Weitkamp, *Stud. Surf. Sci. Catal.*, *105*, 853 (1996).
14. M. Hunger and T. Horvath, *J. Catal.*, *167*, 187 (1997).
15. P. Goguen and J. F. Haw, *J. Catal.*, *161*, 870 (1996).

16. D. B. Ferguson and J. F. Haw, *Anal. Chem.*, *67*, 3342 (1995).
17. M. Hunger, D. Freude, H. Pfeifer, D. Prager, and W. Reschetilowski, *Chem. Phys. Lett.*, *163*, 221 (1989).
18. J. P. Yesinowski and H. Eckert, *J. Am. Chem. Soc.*, *109*, 6274 (1987).
19. M. L. Costenoble, M. J. Mortier, and J. B. Uytterhoeven, *J. Chem. Soc., Faraday Trans. 1*, *174*, 466 (1978); *174*, 477 (1978).
20. U. Lohse, E. Loeffler, M. Hunger, J. Stoeckner, and V. Patzelova, *Zeolites*, *7*, 11 (1987).
21. D. Freude, M. Hunger, and H. Pfeifer, *Z. Phys. Chem. (NF)*, *152*, 429 (1987).
22. M. Hunger, D. Freude, and H. Pfeifer, *Catal. Today*, *3*, 507 (1988).
23. G. Engelhardt, H. G. Jerschkewitz, U. Lohse, P. Sarv, A. Samoson, and E. Lippmaa, *Zeolites*, *7*, 291 (1987).
24. V. M. Mastikhin, I. L. Mudrakovsky, and K. I. Zamaraev, *React. Kinet. Catal. Lett.*, *34*, 161 (1987).
25. H. Koller, R. F. Lobo, S. L. Burkett, and M. E. Davis, *J. Phys. Chem.*, *99*, 12588 (1995).
26. D. Freude, M. Hunger, H. Pfeifer, and W. Schwieger, *Chem. Phys. Lett.*, *128*, 62 (1986).
27. M. Hunger, Thesis (habilitation), Department of Physics, University of Leipzig (1991).
28. M. Hunger, M. W. Anderson, A. Ojo, and H. Pfeifer, *Microporous Mater.*, *1*, 17 (1993).
29. R. T. Sanderson, *Chemical Bonds and Bond Energy*, Academic Press, New York, 1976.
30. E. Brunner, *J. Chem. Soc., Faraday Trans.*, *89*, 165 (1993).
31. M. A. Makarova, A. F. Ojo, K. Karim, M. Hunger, and J. Dwyer, *J. Phys. Chem.*, *98*, 3619 (1994).
32. V. L. Zholobenko, L. M. Kustov, V. Yu. Borovkov, and V. B. Kazansky, *Zeolites*, *8*, 175 (1988).
33. E. Brunner, H. G. Karge, and H. Pfeifer, *Z. Phys. Chem.*, *176*, 173 (1992).
34. L. W. Beck, J. L. White, and J. F. Haw, *J. Am. Chem. Soc.*, *116*, 9657 (1994).
35. E. Brunner, K. Beck, M. Koch, H. Pfeifer, B. Staudte, and D. Zscherpel, *Stud. Surf. Sci. Catal.*, *84*, 357 (1994).
36. E. Brunner, K. Beck, L. Heeribout, and H. G. Karge, *Microporous Mater.*, *3*, 395 (1995).
37. L. W. Beck and J. F. Haw, *J. Phys. Chem.*, *99*, 1076 (1995).
38. M. Hunger, J. Kaerger, H. Pfeifer, J. Caro, B. Zibrowius, M. Buelow, and R. Mostowicz, *J. Chem. Soc., Faraday Trans. 1*, *83*, 3459 (1987).
39. V. M. Mastikhin, I. L. Mudrakovsky, and A. V. Nosov, *Prog. NMR Spectrosc.*, *23*, 259 (1991).
40. E. Brunner, H. Ernst, D. Freude, T. Froehlich, M. Hunger, and H. Pfeifer, *Stud. Surf. Sci. Catal.*, *49*, 623 (1989).
41. B. Staudte, M. Hunger, and M. Nimz, *Zeolites*, *11*, 837 (1991).
42. D. Freude, *Chem. Phys. Lett.*, *235*, 69 (1995).
43. M. Hunger, S. Ernst, S. Steuernagel, and J. Weitkamp, *Microporous Mater.*, *6*, 349 (1996).
44. M. M. Maricq and J. S. Waugh, *J. Chem. Phys.*, *70*, 3300 (1979).

Downloaded By: [University of Stuttgart] At: 16:06 10 September 2009

45. E. Brunner, D. Fenzke, D. Freude, and H. Pfeifer, *Chem. Phys. Lett.*, *169*, 591 (1990).
46. R. A. Wind, in *Modern NMR Techniques and Their Application in Chemistry* (A. I. Popov and K. Hallenga, eds.), Marcel Dekker, Inc., New York, 1991, p. 125.
47. A. Abragam, *Principles of Nuclear Magnetism*, Clarendon Press, Oxford, 1994.
48. E. Brunner, *J. Chem. Soc., Faraday Trans.*, *86*, 3957 (1990).
49. E. Brunner, D. Freude, B. C. Gerstein, and H. Pfeifer, *J. Magn. Reson.*, *90*, 90 (1990).
50. U. Haeberlen and J. S. Waugh, *Phys. Rev.*, *175*, 453 (1968).
51. B. Schnabel, U. Haubenreisser, G. Scheler, and R. Mueller, *Proc. 19th Congr. AMPERE*, Springer-Verlag, Berlin, 1976, p. 441.
52. R. G. Pembleton, L. M. Ryan, and B. C. Gerstein, *Rev. Sci. Instrum.*, *48*, 1286 (1977).
53. L. M. Ryan, R. E. Taylor, A. J. Paff, and B. C. Gerstein, *J. Chem. Phys.*, *72*, 508 (1980).
54. G. Scheler, U. Haubenreisser, and H. Rosenberger, *J. Magn. Reson.*, *44*, 134 (1981).
55. E. R. Andrew and A. Jasinski, *J. Phys. C: Solid State Phys.*, *4*, 391 (1971).
56. D. Fenzke, B. C. Gerstein, and H. Pfeifer, *J. Magn. Reson.*, *98*, 469 (1992).
57. J. Boehm, D. Fenzke, and H. Pfeifer, *J. Magn. Reson.*, *55*, 197 (1983).
58. A. C. Olivieri, L. Frydman, and L. E. Diaz, *J. Magn. Reson.*, *75*, 50 (1987).
59. A. C. Olivieri, *J. Magn. Reson.*, *81*, 201 (1989).
60. A. C. Olivieri, *J. Magn. Reson. A*, *101*, 313 (1993).
61. M. Alla and E. Lippmaa, *Chem. Phys. Lett.*, *87*, 30 (1982).
62. I. D. Gay, *J. Magn. Reson.*, *58*, 413 (1984).
63. C. E. Bronnimann, I.-S. Chuang, and B. L. Hawkins, *J. Am. Chem. Soc.*, *109*, 1562 (1987).
64. G. L. Woolery, L. B. Alemany, R. M. Dessau, and A. W. Chester, *Zeolites*, *6*, 14 (1986).
65. J. W. Ward, *J. Catal.*, *9*, 225 (1969).
66. J. W. Ward and R. C. Hansford, *J. Catal.*, *13*, 364 (1969).
67. Z. Jirak, S. Vratislav, and V. Bosacek, *J. Phys. Chem. Solids*, *41*, 1089 (1980).
68. M. Czjzek, H. Jobic, A. N. Fitch, and T. Voigt, *J. Phys. Chem.*, *96*, 1535 (1992).
69. D. W. Breck, *Zeolite Molecular Sieve*, Robert E. Krieger, Malabar, FL, 1984.
70. J. W. Ward, in *Zeolite Chemistry and Catalysis* (J. A. Rabo, ed.), ACS Monograph 171, American Chemical Society, Washington, DC, 1976, p. 118.
71. E. Brunner, *Microporous Mater.*, *1*, 431 (1993).
72. A. E. Hirschler, *J. Catal.*, *2*, 428 (1963).
73. C. J. Plank, *Proc. 3rd Int. Congr., Vol. 1*, North-Holland, Amsterdam, 1963, p. 727.
74. D. Freude, T. Froehlich, M. Hunger, H. Pfeifer, and G. Scheler, *Chem. Phys. Lett.*, *98*, 263 (1983).
75. G. H. Kuehl, *Proc. 3rd Int. Conf. Molecular Sieves*, Leuven University Press, Leuven, 1973, p. 227.

Downloaded By: [University of Stuttgart] At: 16:06 10 September 2009

76. J. B. Uytterhoeven, L. G. Christner, and W. K. Hall, *J. Phys. Chem.*, *69*, 2177 (1965).
77. E. Brunner, H. Ernst, D. Freude, T. Froehlich, M. Hunger, and H. Pfeifer, *J. Catal.*, *127*, 34 (1991).
78. R. M. Lago, W. O. Haag, R. J. Mikovsky, D. H. Olson, S. D. Hellring, K. D. Schmitt, and G. T. Kerr, *Stud. Surf. Sci. Catal.*, *28*, 677 (1986).
79. J. Klinowski, H. Hamdan, A. Corma, V. Fornes, M. Hunger, and D. Freude, *Catal. Lett.*, *3*, 263 (1989).
80. W. Reschetilowski, W. D. Einicke, M. Jusek, R. Schoellner, D. Freude, M. Hunger, and J. Klinowski, *Appl. Catal.*, *56*, L15 (1989).
81. U. Fleischer, W. Kutzelnigg, A. Bleiber, and J. Sauer, *J. Am. Chem. Soc.*, *115*, 7833 (1993).
82. H. Ernst, D. Freude, and I. Wolf, *Chem. Phys. Lett.*, *212*, 588 (1993).
83. D. Freude, H. Ernst, and I. Wolf, *Solid State Nucl. Magn. Reson.*, *3*, 271 (1994).
84. B. Berglund and R. W. Vaughan, *J. Chem. Phys.*, *73*, 2037 (1980).
85. U. Sternberg and E. Brunner, *J. Magn. Reson. A*, *108*, 142 (1994).
86. M. Hunger, D. Freude, T. Froehlich, H. Pfeifer, and W. Schwieger, *Zeolites*, *7*, 108 (1987).
87. T. Ikenoue and N. Yoshida, *J. Phys. Chem.*, *92*, 4883 (1988).
88. J. H. Lunsford, W. P. Rothwell, and W. Shen, *J. Am. Chem. Soc.*, *107*, 1540 (1985).
89. J. H. Lunsford, P. N. Tutunjian, P.-J. Chu, E. B. Yeh, and D. J. Zalewski, *J. Phys. Chem.*, *93*, 2590 (1989).
90. L. Baltusis, J. S. Frye, and G. E. Maciel, *J. Am. Chem. Soc.*, *109*, 40 (1987).
91. A. I. Biaglow, R. J. Gorte, G. T. Kokotailo, and D. White, *J. Catal.*, *148*, 779 (1994).
92. J. L. White, L. W. Beck, and J. F. Haw, *J. Am. Chem. Soc.*, *114*, 6182 (1992).
93. J. F. Haw, M. B. Hall, A. E. Alvarado-Swaisgood, E. J. Munson, Z. Lin, L. W. Beck, and T. Howard, *J. Am. Chem. Soc.*, *116*, 7308 (1994).
94. M. Koch, E. Brunner, D. Fenzke, H. Pfeifer, and B. Staudte, *Stud. Surf. Sci. Catal.*, *84*, 709 (1994).
95. H. Sachsenroeder, E. Brunner, M. Koch, H. Pfeifer, and B. Staudte, *Microporous Mater.*, *6*, 341 (1996).
96. E. A. Paukshtis and E. N. Yurchenko, *Usp. Khim.*, *52*, 426 (1983).
97. E. A. Paukshtis and E. N. Yurchenko, *React. Kinet. Catal. Lett.*, *16*, 131 (1981).
98. B. Zibrowius, E. Loeffler, and M. Hunger, *Zeolites*, *12*, 167 (1992).
99. W. M. Meier, D. H. Olson, and Ch. Baerlocher, *Atlas of Zeolite Structure Types*, Elsevier, London, 1996.
100. M. Hunger, Plenary lecture, *8th German Zeolite Conference*, Berlin, 1996.
101. D. Michel and F. Engelke, *NMR Basic Principles Prog.*, *32*, 69 (1994).
102. S. R. Hartmann and E. L. Hahn, *Phys. Rev.*, *128*, 2042 (1962).
103. G. Engelhardt, U. Lohse, A. Samoson, M. Maegi, M. Tarmak, and E. Lippmaa, *Zeolites*, *2*, 59 (1982).
104. R. R. Ernst, *Chimia*, *41*, 323 (1987).
105. D. Freude, H. Ernst, M. Hunger, H. Pfeifer, and E. Jahn, *Chem. Phys. Lett.*, *143*, 477 (1988).

Downloaded By: [University of Stuttgart] At: 16:06 10 September 2009

106. G. Engelhardt, B. Fahlke, M. Maegi, and E. Lippmaa, *Z. Phys. Chem. (NF), 266*, 239 (1985).
107. W. Schwieger, K. H. Bergk, D. Freude, M. Hunger, and H. Pfeifer, *ACS Symp Ser., 398*, 274 (1989).
108. M. Hunger, D. Freude, H. Pfeifer, and W. Schwieger, *Chem. Phys. Lett., 167*, 21 (1990).
109. N. Van-Den-Begin, L. V. C. Rees, J. Caro, M. Buelow, M. Hunger, and J. Kaerger, *J. Chem. Soc., Faraday Trans. 1, 85*, 1501 (1989).
110. E. J. J. Groenen, A. G. T. G. Kortbeek, M. Mckay, and O. Sudmeijer, *Zeolites, 6*, 403 (1986).
111. D. Freude, W. Oehme, H. Schmiedel, and B. Staudte, *J. Catal., 32*, 137 (1974).
112. T. Baba, Y. Inoue, H. Shoji, T. Uematus, and Y. Ono, *Microporous Mater., 3*, 647 (1995).
113. P. Sarv, T. Tuherm, E. Lippmaa, K. Keskinen, and A. Root, *J. Phys. Chem., 99*, 13763 (1995).
114. H. Schaefer, Thesis (diploma), Department of Physics, University of Leipzig (1987).
115. P. W. Anderson and P. R. Weiss, *Jpn. J. Phys. Soc., 9*, 316 (1954).
116. B. Schneider, D. Doskocilova, and J. Jakes, *Proc. 20th Congr. AMPERE*, Springer-Verlag, Berlin, 1979, p. 57.
117. R. A. van Santen, *Stud. Surf. Sci. Catal., 85*, 273 (1994).
118. J. Sauer, *Stud. Surf. Sci. Catal., 84*, 2039 (1994).
119. K. P. Schroeder, J. Sauer, M. Leslie, C. R. A. Catlow, and J. M. Thomas, *Chem. Phys. Lett., 188*, 320 (1992).
120. L. A. Curtiss, H. Brand, J. B. Nicholas, and L. E. Iton, *Chem. Phys. Lett., 184*, 215 (1991).
121. D. Freude, J. Klinowski, and H. Hamdan, *Chem. Phys. Lett., 149*, 355 (1988).
122. D. Freude and J. Klinowski, *J. Chem. Soc., Chem. Commun.*, 1411 (1988).
123. N. P. Kenaston, A. T. Bell, and J. A. Reimer, *J. Phys. Chem., 98*, 894 (1994).
124. D. Fenzke, M. Hunger, and H. Pfeifer, *J. Magn. Reson., 95*, 477 (1991).
125. M. Hunger, D. Freude, D. Fenzke, and H. Pfeifer, *Chem. Phys. Lett., 191*, 391 (1992).
126. W. P. Aue, D. J. Ruben, and R. G. Griffin, *J. Magn. Reson., 43*, 472 (1981).
127. L. M. Bull, A. K. Cheetham, P. D. Hopkins, and B. M. Powell, *J. Chem. Soc., Chem. Commun.*, 1196 (1993).
128. S. Beran, *J. Mol. Catal., 10*, 177 (1981).
129. S. Beran, *J. Phys. Chem., 87*, 55 (1983).
130. P. Geerlings, N. Tariel, A. Botrel, R. Lissilour, and W. J. Mortier, *J. Phys. Chem., 88*, 5752 (1984).
131. M. Koch, E. Brunner, H. Pfeifer, and D. Zscherpel, *Chem. Phys. Lett., 228*, 501 (1994).
132. M. Hunger, T. Horvath, G. Engelhardt, and H. G. Karge, *Stud. Surf. Sci. Catal., 94*, 756 (1995).
133. M. Hunger and T. Horvath, *Ber. Bunsenges. Phys. Chem., 99*, 1316 (1995).
134. M. Hunger and T. Horvath, *J. Am. Chem. Soc., 118*, 12302 (1996).
135. D. Engelhardt, S. Luger, J. Ch. Buhl, and J. Felsche, *Zeolites, 9*, 192 (1989).
136. C. A. Fyfe, Y. Feng, and H. Grondey, *Microporous Mater., 1*, 393 (1993).
137. R. Radeglia and G. Engelhardt, *Chem. Phys. Lett., 114*, 28 (1985).

Downloaded By: [University of Stuttgart] At: 16:06 10 September 2009

138. J. Sauer, *Chem. Rev.*, *89*, 199 (1989).
139. E. Kassab, K. Seiti, and M. Allavena, *J. Phys. Chem.*, *92*, 6705 (1988); *95*, 9425 (1991).
140. D. Freude and J. Haase, *NMR Basic Principles Prog.*, *29*, 1 (1993).
141. S. Ghose and T. Tsang, *Am. Mineral.*, *58*, 748 (1973).
142. J. Skibsted, P. Norby, H. Bilsøe, and H. J. Jakobsen, *Solid State Nucl. Magn. Reson.*, *5*, 239 (1995).
143. G. Engelhardt and W. Veeman, *J. Chem. Soc., Chem. Commun.*, 622 (1993).
144. F. Haase and J. Sauer, *J. Phys. Chem.*, *98*, 3083 (1994).
145. F. Haase and J. Sauer, *J. Am. Chem. Soc.*, *117*, 3780 (1995).
146. J. D. Gale, C. R. A. Catlow, and J. R. Carruthers, *Chem. Phys. Lett.*, *216*, 155 (1993).
147. E. Nusterer, P. E. Boechl, and K. Schwarz, *Angew. Chem. Int. Ed. Engl.*, *35*, 175 (1996).
148. M. W. Anderson, P. J. Barrie, and J. Klinowski, *J. Phys. Chem.*, *95*, 235 (1991).
149. G. Mirth, J. A. Lercher, M. W. Anderson, and J. Klinowski, *J. Chem. Soc., Faraday Trans. 1*, *86*, 3039 (1990).
150. A. Thursfield and M. W. Anderson, *J. Phys. Chem.*, *100*, 6698 (1996).
151. M. Krossner and J. Sauer, *J. Phys. Chem.*, *100*, 6199 (1996).
152. J. F. Haw, in *NMR Techniques in Catalysis* (A. T. Bell and A. Pines, eds.), Marcel Dekker, Inc., New York, 1994, p. 139.
153. J. Klinowski, *Chem. Rev.*, *91*, 1459 (1991).
154. J. Klinowski, *Anal. Chimi. Acta*, *283*, 929 (1993).
155. I. I. Ivanova and E. G. Derouane, *Stud. Surf. Sci. Catal.*, *85*, 357 (1994).
156. H. Pfeifer and H. Ernst, *Annu. Rept. NMR Spectrosc.*, *28*, 91 (1994).
157. P. A. Jacobs, M. Tielen, and J. B. Uytterhoeven, *J. Catal.*, *50*, 98 (1977).
158. P. A. Jacobs and J. B. Uytterhoeven, *J. Catal.*, *50*, 109 (1977).
159. S. J. Gentry and R. Rudham, *J. Chem. Soc., Faraday Trans. 1*, *70*, 1685 (1974).
160. R. Rudham, A. I. Spiers, and A. W. Winstanley, *Zeolites*, *11*, 850 (1991).
161. M. J. Hey, A. Nock, R. Rudham, I. P. Appleyard, G. A. J. Haines, and R. K. Harries, *J. Chem. Soc., Faraday Trans. 1*, *82*, 2817 (1986).
162. M. Hunger, D. Freude, and H. Pfeifer, *J. Chem. Soc., Faraday Trans.*, *87*, 657 (1991).
163. P. Batamack, C. Doremieux-Morin, J. Fraissard, and D. Freude, *J. Phys. Chem.*, *95*, 3790 (1991).

Downloaded By: [University of Stuttgart] At: 16:06 10 September 2009

Downloaded By: [University of Stuttgart] At: 16:06 10 September 2009